Erstgutachterin: PD Dr. Jeanette Lorenz
Zweitgutachter: Prof. Dr. Wolfgang Dünnweber

Search for charginos and neutralinos in a signature with a Higgs boson and an isolated lepton with the ATLAS detector and its reinterpretation in the phenomenological MSSM

Thesis submitted for a doctoral degree in physics
at the faculty of physics of the
Ludwig-Maximilians University
Munich, Germany

Submitted by Eric Schanet, born in Luxembourg
on May 4th, 2021

Part I

Fundamental concepts

Part II

The 1-lepton analysis

Part III

Reinterpretation

Chapter 10

Simplified likelihoods

In the previous chapter, the concept of preserving an analysis for the purpose of reinterpretations was introduced and a truth-level version of the signal pipeline was discussed. In large-scale reinterpretations involving a large number of Supersymmetry (SUSY) models to be tested against, not only the signal pipeline, but also the statistical inference requires significant computational effort. This chapter introduces the concept of *simplified likelihoods*, a method approximating the statistical model of an analysis using the HistFactory template in order to achieve more efficient profile likelihood fits and, ultimately, hypothesis tests [289].

10.1   Motivation

Reinterpretations of ATLAS searches for SUSY in more complete and realistic SUSY scenarios (as opposed to simplified models) typically involve high-dimensional parameter spaces that are computationally extremely challenging to sample and compare to ATLAS data in an exhaustive manner. Large-scale reinterpretations of this type have already been performed by the ATLAS Collaboration after the Run 1 data-taking period in both the full 19-dimensional phenomenological Minimal Supersymmetric Standard Model (pMSSM) [87], as well as in a 5-dimensional representation of the pMSSM focussing on the electroweak sector [86]. Due to the complexity of the statistical models of ATLAS searches for SUSY, originating from the large number of channels and the sizeable set of nuisance parameters usually considered[†], the wall time needed for the statistical inference is usually not negligible. In a typical large-scale reinterpretation involving $\mathcal{O}(10^5 - 10^6)$ sampled models, an optimistic estimation of the wall time needed for the statistical inference per model of $\mathcal{O}(10\,\mathrm{s} - 10^2\,\mathrm{s})$ is too computationally expensive, especially when more than just a single ATLAS search is included. It is thus crucial to reduce the number of models that need to be evaluated using the searches' full statistical model.

One approach of alleviating this computational problem is to approximate the SUSY searches through their model-independent upper limits, often published in conjunction with the model-dependent exclusion limits. As discussed in section 5.3, the model-independent upper limits are derived using single-bin signal regions that do not rely on shape-fits, but simply count the number of events after a set of selection cuts (so-called *cut-and-count* regions), thereby making minimal model assumptions. In

---

[†]   As an example, the full likelihood of the 1ℓ search using the exclusion signal regions has 8 channels with a total of 14 bins. Each channel contains event rates for 9 samples that depend on a total of 115 modifiers.
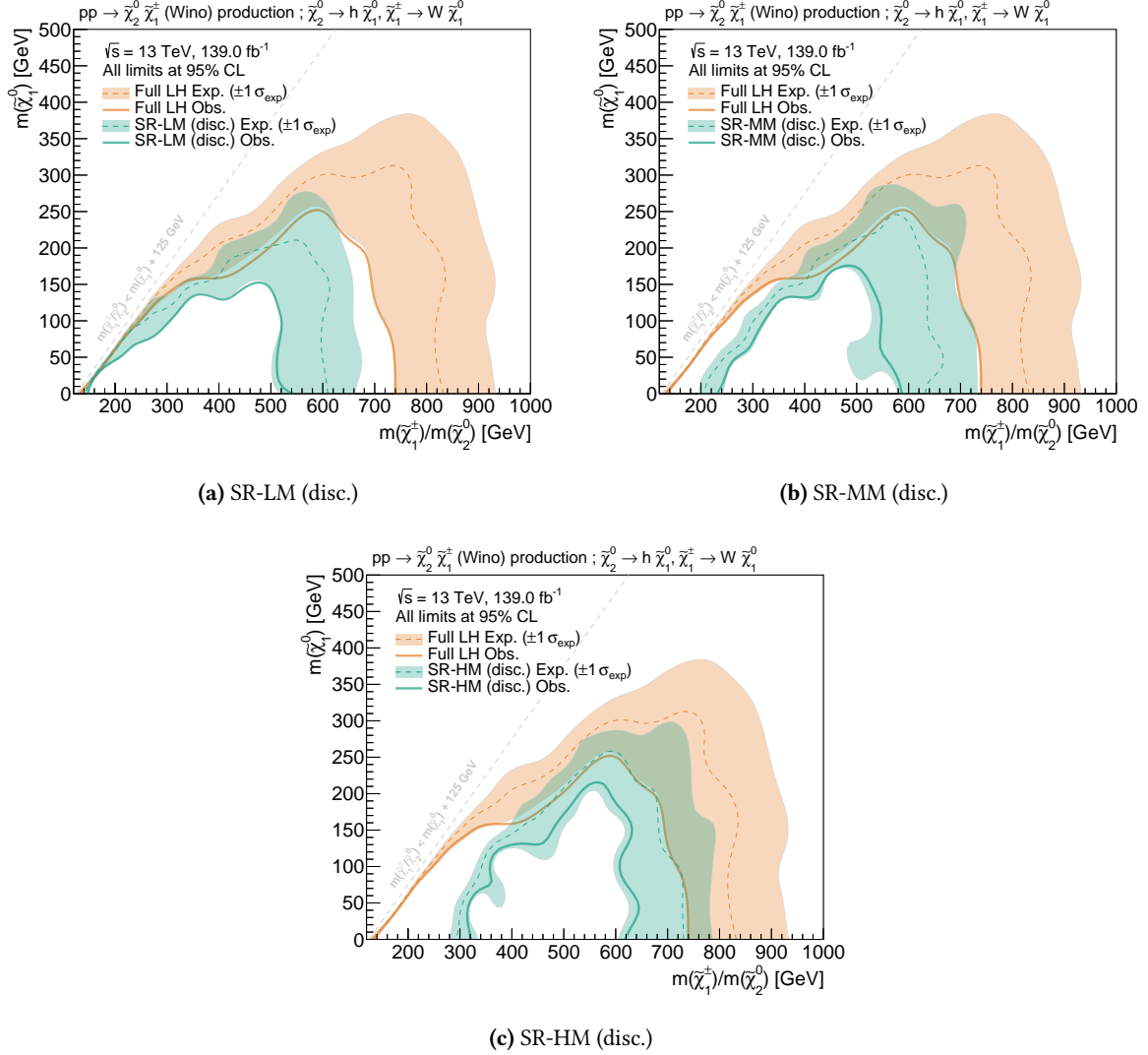
(a) SR-LM (disc.)

(b) SR-MM (disc.)

(c) SR-HM (disc.)

Figure 10.1: Comparison of exclusion limits obtained using the likelihood built from all nine exclusion signal regions (orange), and the discovery signal regions (green). As discussed in section 5.3, the discovery signal regions are simple *cut-and-count* regions making minimal model assumptions. They are not mutually exclusive and, therefore, cannot be statistically combined, resulting in three separate exclusion contours. The full set of statistical and systematic uncertainties on the background and the signal event rates are included in all regions. The shorthand notation 'LH' refers to likelihood.

the case of searches using dedicated multi-bin signal regions that are statistically combined to derive exclusion limits on model parameters, this approach—while computationally very efficient—naturally underestimates the true exclusion power of the respective search because model-dependent signal shapes are not exploited.

Figure 10.1 illustrates this approach in the context of the 1ℓ search. The exclusion limits, obtained with the exclusion signal regions implementing a two-dimensional shape-fit, are compared to the exclusion contours obtained using the discovery signal regions, defined in table 5.3. As the discovery signal regions are not mutually exclusive, they cannot be statistically combined and thus three separate observed and expected contours need to be drawn. It is straightforward to observe that even a best-expected combination of the three exclusion contours obtained from the discovery signal regions does not reach the sensitivity achieved using the two-dimensional shape-fit setup. Due to a lack of alternative, equally computationally efficient approaches, this procedure was, in the past, nonetheless used in large-scale scans of the pMSSM using ATLAS data from Run 1 [87, 86]. The results obtained were therefore somewhat conservative, leaving substantial room for improvement.

In summary, this motivates the introduction of a method for approximating ATLAS searches for SUSY without disregarding their elaborate use of multi-bin signal regions exploiting the varying shapes of signal and Standard Model (SM) background distributions. The method introduced hereafter targets ATLAS searches for SUSY using likelihoods built according to the HistFactory template.

10.2   Building simplified likelihoods

In order to retain the full statistical combination of multiple signal region bins implemented in many SUSY searches, while still being able to achieve a sufficiently fast approximation, the statistical treatment of the background model including its uncertainties needs to be simplified. In the procedure presented in the following, this is achieved by first performing a background-only fit to data using the full likelihood in order to determine the best-fit values of all model parameters ϕ. The post-fit total background estimates as well as the total uncertainty on the estimates in every bin are subsequently computed from the best-fit values, and used to construct a simplified likelihood.

As the full likelihood in JSON format defines the full statistical model used for the statistical inference, the above background-only fit can be performed using pyhf and the preserved likelihood of the analysis. With the full likelihoods starting to become available on HEPDATA (see e.g. Ref. [277]) this procedure can rely on public information only and is therefore widely accessible to the high energy physics (HEP) community. For this reason, the simplified likelihoods introduced herein adhere to the same JSON specification used for the full likelihoods, described in detail in Ref. [162]. The following description highlights the specification details relevant to the simplified likelihood.

Background model

In the simplified likelihood, the background model is approximated with a single background sample, representing the total SM background estimate in the different analysis channels. The pre-fit sample rate of the total background sample in the simplified likelihood is set to the total post-fit background estimate obtained in the background-only fit using the full likelihood. Furthermore, the complete set of nuisance parameters in the original full likelihood is reduced to a single constrained parameter with up and down variations corresponding to the post-fit uncertainties on the total SM background

estimates in each bin. It is constrained by a Gaussian of the form $\text{Gaus}(a = 0, \sigma = 1)$ and is correlated over all bins in each channel. The 1σ up and down evaluations of the rate modification, necessary for the interpolations during the profile likelihood fit to data, are given by the post-fit uncertainties on the total background estimate. Although the final uncertainty is thus constrained by a simple Gaussian, non-Gaussian effects are included to some extent due to the full treatment of the uncertainties in the full likelihood fit, performed in order to derive the pre-fit values for the simplified likelihood.

Listing 10.1 shows an exemplary total background sample, called 'total_bkg', defining expected event rates for a channel with three bins. The single nuisance parameter is called 'total_error' and is implemented as a *rate modifier* (cf. section 3.1).

```
{
  "name": "total_bkg",
  "data": [6.44, 4.62, 1.60],
  "modifiers": [{
    "data": {
      "hi_data": [8.43, 6.04, 2.23],
      "lo_data": [4.45, 3.19, 0.97]
    },
    "name": "total_error",
    "type": "histosys"
  }]
}
```

Listing 10.1: Exemplary total background sample with sample rate and total uncertainty for three separate bins, derived from a fit in the signal regions (SRs) and control regions (CRs) using the full likelihood. The histosys type modifier in HistFactory implements a shape uncertainty correlated over all bins.

Analysis channels

Each channel in the full likelihood with the original number of bins is also entering the simplified likelihood[†]. Each contains a total background sample as specified above. Apart from the total background sample, one additional sample is needed: the signal sample. It introduces the unconstrained signal strength parameter μ as second and final parameter of the likelihood. In the hypothesis tests, the signal strength parameter acts as Parameter of Interest (POI).

As an example, the channel definition of the exclusion signal region SR-HM in the simplified likelihood of the 1ℓ search is shown in listing 10.2. For simplicity, the exemplary signal sample does not introduce any additional uncertainties on the signal rates, thereby assuming them to be negligible. Depending on the beyond the Standard Model (BSM) scenario, signal uncertainties can, however, be introduced through additional event rate modifiers.

[†] Being able to reproduce the full statistical combination of all analysis regions is one of the main motivations for the introduction of the simplified likelihood.

```json
{
  "name": "SR-HM",
  "samples": [
    {
      "name": "total_bkg",
      ...
    },
    {
      "name": "signal",
      "data": [2.3, 5.8, 7.1],
      "modifiers": [{
        "data": null,
        "name": "mu",
        "type": "normfactor"
      }]
    }
  ]
}
```

Listing 10.2: Channel definition of the exclusion signal region SR-HM of the 1ℓ search. The exemplary signal sample with sample rate and unconstrained normalisation parameter does not introduce any additional uncertainties. The three dots '…' contain the remaining definition for the total background sample from listing 10.1.

Observations and measurements

According to the JSON specification defined in Ref. [162], the data observed by the analysis in each channel (and each bin) is introduced by means of an *observation*. In the case of the simplified likelihood, this is taken directly from the full likelihood and, by construction, does not need to be modified in any form. An example of an observation including several channels and bins is shown in listing 10.3.

```json
{
  "observations": {
    {
      "name": "SR-HM",
      "data": [6.0, 5.0, 3.0]
    },
    \dots
  }
}
```

Listing 10.3: Example of an observation in the simplified likelihood, taken directly from the full likelihood of the 1ℓ search. The number of events observed in data are given for each bin in the exclusion signal region SR-HM. Similar entries exist for all other regions, indicated by the dots '…'.

The only part of the JSON specification left to be defined is the *measurement*, specifying the name of the parameter of interest as well as parameter set configurations not already covered in the channel definitions. For the simplified likelihood, it is straightforward to write down, as the POI is the signal strength parameter and no additional parameters need further configuration.

Put together, the above pieces result in a simplified likelihood for a given signal model, using a background model obtained from an initial background-only fit using the full likelihood, thus considering the full treatment of the systematic uncertainties. The simplified likelihood approach therefore assumes
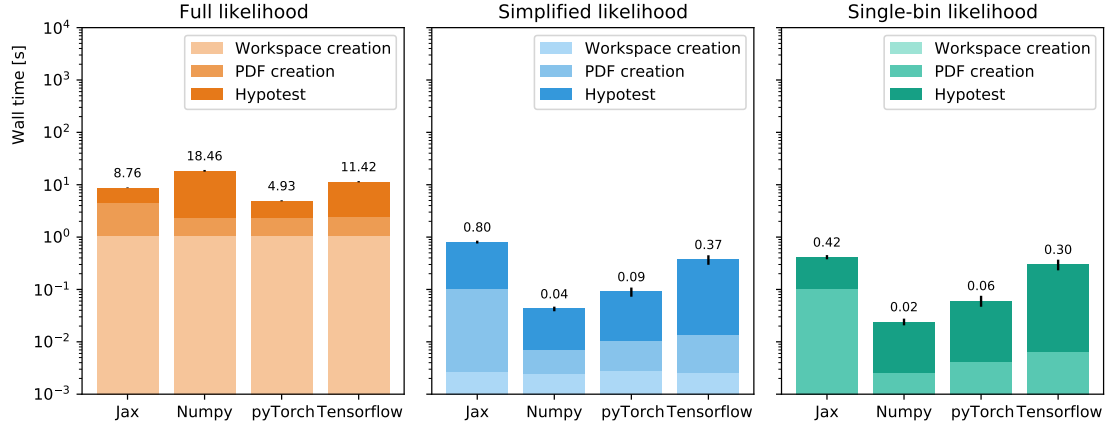
Figure 10.2: Benchmarks of the wall times for hypothesis testing using different likelihoods and `pyhf` backends in the context of the 1ℓ search. Benchmarking details are given in the text. The full likelihood (left) includes the full statistical implementation of the original analysis, the simplified likelihood (center) represents the simplified likelihood approach presented in this document, and the single-bin likelihood (right) represents the single-bin approximation using the discovery signal regions. The '*workspace creation*' refers to I/O operations reading in the `JSON` file containing the likelihood. The '*pdf creation*' step refers to the creation of the statistical model in a `pyhf`-internal structure. '*Hypotest*' refers to the wall time of a single exclusion hypothesis test computing a CL_s value. The error bars correspond to the standard deviation of the benchmark sample.

the total background estimate to be fixed at the post-fit values obtained from the initial full likelihood fit, and, furthermore, only allows the background estimates to vary within the total uncertainty.

All simplified likelihoods used in the following have been produced using Simplify [290], a `python` tool written by the author. The background model of the simplified likelihood of the 1ℓ search in `JSON` format is available at Ref. [291]. By the means of `JSON` patches [292], any signal model, for which the nominal expected event rates in the analysis regions are known, can then be evaluated using this simplified likelihood.

10.3 Computational performance

One of the main figures of merit of an analysis approximation obviously is the reduction in computational wall time compared to the full analysis. Figure 10.2 shows the results of a benchmark for different likelihood configurations in the context of the 1ℓ search. The wall times of hypothesis tests using the full analysis likelihood are compared with those using the simplified likelihood constructed following the previously introduced prescription. In addition, the wall time of the single-bin likelihood relying on the discovery SRs, already used in fig. 10.1, is shown. For each likelihood, different computational backends are exploited for the tensor algebra operations in `pyhf`. All benchmarks have been performed on an Intel i7-4790 CPU with a nominal clock speed of 3.60 GHz, 4 cores and 8 threads. The CPU was not isolated, but under minimal load. The original 125 signal points of the 1ℓ search were used in each configuration.

The use of automatic differentiation of the full log-likelihood gradient, enabled by some of the tensor algebra backends to `pyhf`, offers an efficient minimisation of the negative log-likelihood, resulting in fast hypothesis tests of $\mathcal{O}(5\,\text{s})$ for the full likelihood. In large-scale reinterpretations, this is however

Table 10.1: Benchmarks of the wall times needed for computing the CL_s value for a single signal model using the full and the simplified likelihoods. The uncertainty corresponds to the standard deviation of the wall times of the benchmark sample. The performance gain is stated as ratio between the wall times. The PyTorch (NumPy) backend of `pyhf` is used for the full (simplified) likelihood, in conjunction with the SciPy optimiser. Searches without reference quoted were not yet public at the time of writing.

Analysis	Full likelihood [s]	Simplified likelihood [s]	Improvement
ATLAS compressed search [91]	16.49 ± 3.16	0.073 ± 0.012	$236\times$
ATLAS 3ℓ search	40.41 ± 15.7	0.082 ± 0.021	$495\times$
ATLAS 2ℓ search [260]	5.93 ± 0.16	0.079 ± 0.0082	$75\times$
ATLAS 1ℓ search [185]	4.93 ± 0.11	0.040 ± 0.0057	$123\times$
ATLAS direct stau search [293]	1.91 ± 0.090	0.039 ± 0.0055	$49\times$
ATLAS sbottom search [294]	1.36 ± 0.067	0.038 ± 0.0046	$36\times$
ATLAS stop search	2.27 ± 0.062	0.044 ± 0.011	$51\times$

still too computationally expensive. The simplified likelihood, on the other hand, yields minimum wall times for hypothesis tests of the order of 0.04 s per signal model. Compared to the naive single-bin approach using the discovery signal regions (the *single-bin likelihood*), the simplified likelihood thus offers hypothesis tests with a similar wall time[†], but a significantly better approximation of the true analysis exclusion power.

Interestingly, the wall time of the simplified likelihood does not benefit from the usage of features like automatic differentiation, offered by computational backends like PyTorch. This is due to the extreme simplicity of the simplified likelihood function, causing the computational benefits from features like automatic differentiation to not outweigh the sizeable overhead associated to the startup and execution times of tensor algebra libraries like PyTorch.

In addition to the 1ℓ search, the simplified likelihood approach is validated using a larger set of ATLAS searches for SUSY. Table 10.1 summarises the mean wall times of all ATLAS searches investigated. In all cases, PyTorch offers the fastest backend for the full likelihood while NumPy shows best performance for the simplified likelihood. The performance improvement of roughly two orders of magnitude, observed in the 1ℓ search, is confirmed in the remaining ATLAS SUSY searches investigated. The wall time of the simplified likelihoods appears to be bound from below at $\mathcal{O}(10^{-2}\,\mathrm{s})$, limiting the performance gain for some of the faster analyses whose full likelihoods are already relatively simple to begin with.

10.4   Physics performance

A comparison of the exclusion contours, obtained with the full and simplified likelihoods in the context of the 1ℓ search, is shown in fig. 10.3. The results obtained using the simplified likelihood are shown in blue, while the results obtained using the full likelihood are given in orange. Both the observed (without the usual theoretical up and down variations on the signal cross section) and expected exclusion limits including the uncertainty band are shown. In the case of the full likelihood, the complete set of Monte

---

[†]   In fact, the simplified likelihood is even faster than the single-bin approach, as the latter needs to be executed separately for each discovery SR and thus the numbers quoted need to be multiplied by the number of discovery SRs used in the analysis (three in the case of the 1ℓ search).
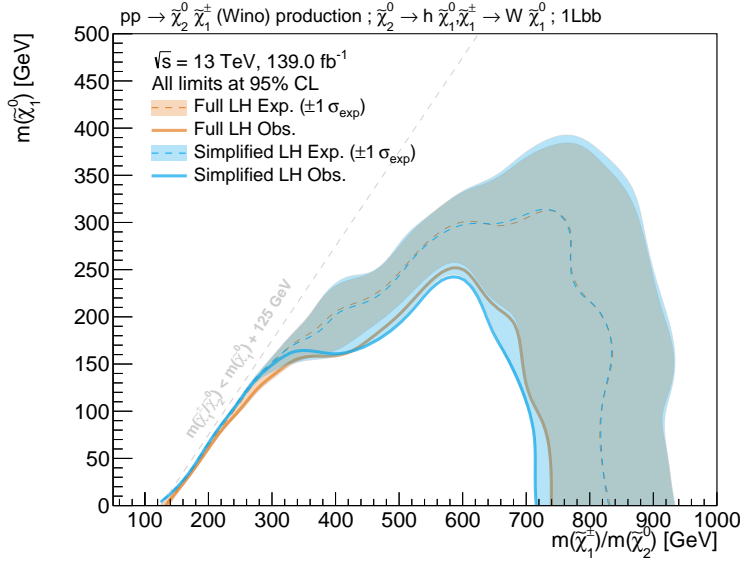
Figure 10.3: Comparison of the exclusion contours obtained with the simplified likelihood (blue) and the full likelihood (orange) of the 1ℓ search. The uncertainty band includes all MC statistical and systematic uncertainties in the case of the full likelihood, and only the simplified uncertainties in the case of the simplified likelihood. The shorthand notation '*LH*' refers to likelihood.

Carlo (MC) statistical and systematic uncertainties, introduced in chapter 7, are taken into account. As discussed in section 10.2, the uncertainty band on the simplified likelihood contour results from the single nuisance parameter, built through reduction of the original nuisance parameters.

The observed and expected CL_s values, obtained using both likelihoods, are shown in fig. 10.4. As expected from the exclusion contour, both the simplified and the full likelihood agree reasonably well across the majority of the CL_s range. For signal models well within exclusion (i.e. $\mathrm{CL}_s \ll 0.05$) according to the full likelihood, the simplified likelihood of the 1ℓ search tends to result in slightly lower CL_s values, yielding a slightly too optimistic sensitivity estimate. In the range relevant to the exclusion contour at 95% CL (i.e. $\mathrm{CL}_s \approx 0.05$), the results from the simplified likelihood agree well with those from the full likelihood.

In addition to the 1ℓ search, the simplified likelihood approach has been validated on the ATLAS searches for SUSY listed in table 10.1. An overview of the results is shown in fig. 10.5, comparing the exclusion contours obtained with the simplified likelihood against the full analysis results. In some analyses, e.g., the ATLAS sbottom and ATLAS 3ℓ searches, both likelihoods are in excellent agreement. In other analyses, like e.g., the ATLAS direct stau search, the agreement is less impressive but overall still acceptable.

In summary, this validation demonstrates that the simplified likelihood method introduced herein can, in many cases, offer a computationally efficient and reliable approximation of ATLAS searches for SUSY relying on the HistFactory probability density function (pdf) template.

10.5   Limitations

Building a well-performing simplified likelihood is not always as straightforward as described in section 10.2, and some analyses require special care when being approximated. For example, in the case of the ATLAS compressed search [91], shown in fig. 10.5(f), only a subset of the original analysis signal regions are entering the simplified likelihood. Studies have shown this to result in an overall improvement in agreement between the two likelihoods. The straightforward structure of the simplified
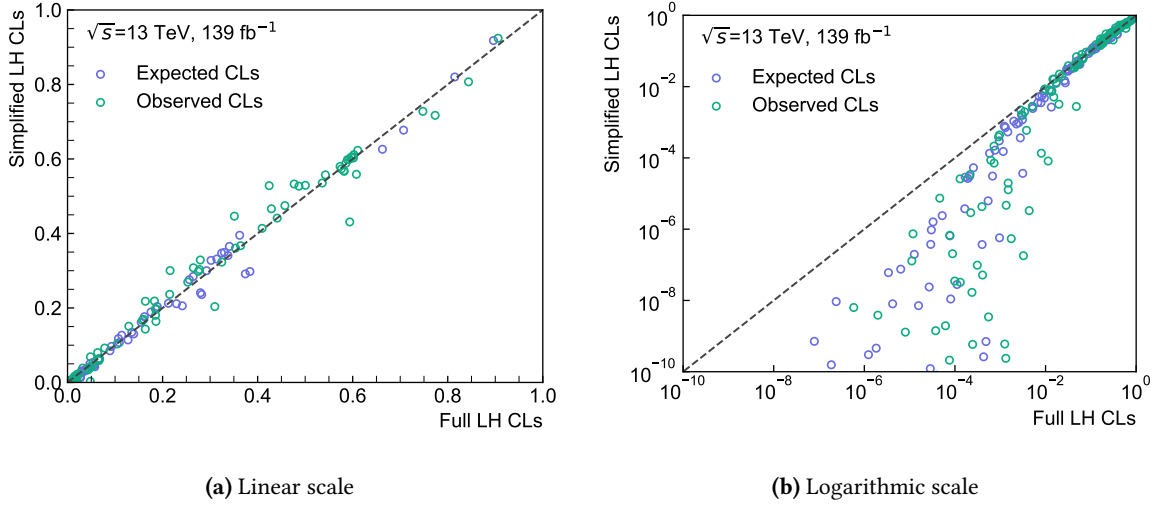
(a) Linear scale

(b) Logarithmic scale

Figure 10.4: Scatter plots comparing the observed and expected CL$_s$ values obtained using the simplified and the full likelihoods for the same set of signal models considered in the 1ℓ search. Both linear and logarithmic scale representations are shown to give an overview of the full range of CL$_s$ values.

likelihood is, in this case, not able to reproduce the statistical behaviour of the background model of the full likelihood in the signal regions omitted. As these signal regions were found to only add limited sensitivity to the search, their removal in the simplified likelihood yields an overall improvement in agreement. Figure B.4 further illustrates the impact of removing these signal regions in the simplified likelihood.

It is worth highlighting again that the simplified likelihood assumes the total background model to be describable by a single sample with a single rate modifier, constrained by a Gaussian and correlated over all bins, with background event rates and uncertainties obtained from a background-only fit using the full likelihood. This, in particular, assumes that the background model is sufficiently constrained by the large statistics in the CRs and that the introduction of signal contributions—especially in the SRs—does not significantly change the background model in a way that cannot be replicated with the simplified likelihood. A configuration, where the background model is no longer mostly constrained by the large statistics in the control regions is tolerable to some extent in the full analysis likelihood, but turns out to be problematic for the simplified likelihood, as it lacks the number of parameters to be able to replicate the behaviour of the full likelihood.

An additional limitation arises in cases of significant signal contamination in the CRs. In the full likelihood, significant signal contaminations in the CRs generally lead to smaller background estimates in the SRs, which, in turn, result in conservative exclusion limits given the observed data. In the simplified likelihood, even with the CRs included, the single constrained nuisance parameter does not offer enough degrees of freedom† to scale down the background model in the $\mu = 1$ hypothesis to the levels obtained in the full likelihood, ultimately resulting in *fake* sensitivity in the CRs. Although it is generally important to limit signal contamination in the CRs for the sake of healthy profile likelihood fits, this is especially true in the case of very simplified likelihoods, like the one introduced

---

† In the full likelihood the normalisation of the SM background is taken care of through floating normalisation parameters (and to some extent other constrained parameters), hence there are more degrees of freedom to fit the model to data.
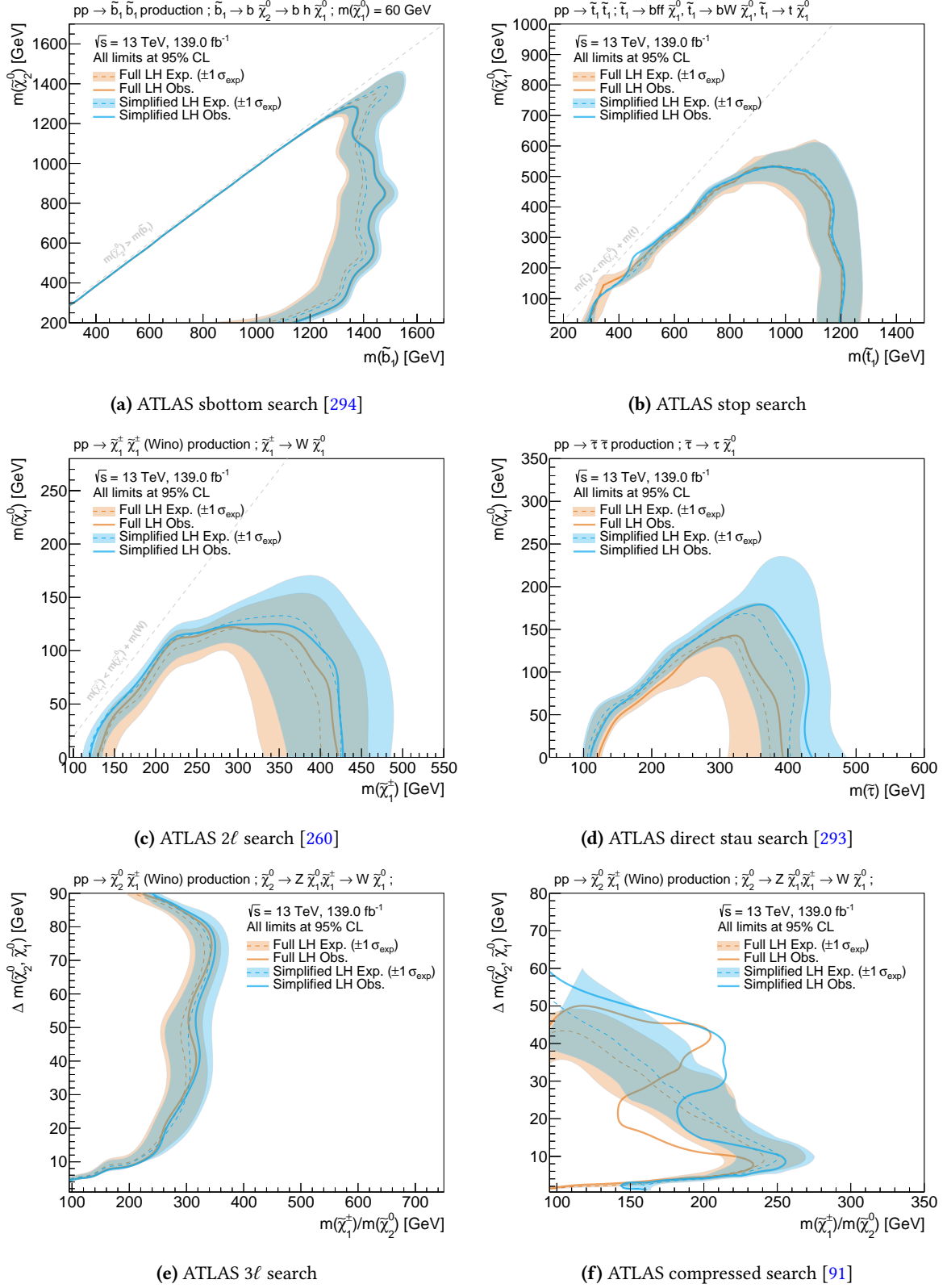
(a) ATLAS sbottom search [294]

(b) ATLAS stop search

(c) ATLAS 2ℓ search [260]

(d) ATLAS direct stau search [293]

(e) ATLAS 3ℓ search

(f) ATLAS compressed search [91]

Figure 10.5: Simplified likelihood results for the different ATLAS searches studied. The results from the simplified likelihood (blue) are compared with the results of the full analysis likelihood (orange). The same reconstruction-level signal inputs are used in both cases. The shorthand notation '*LH*' refers to likelihood.
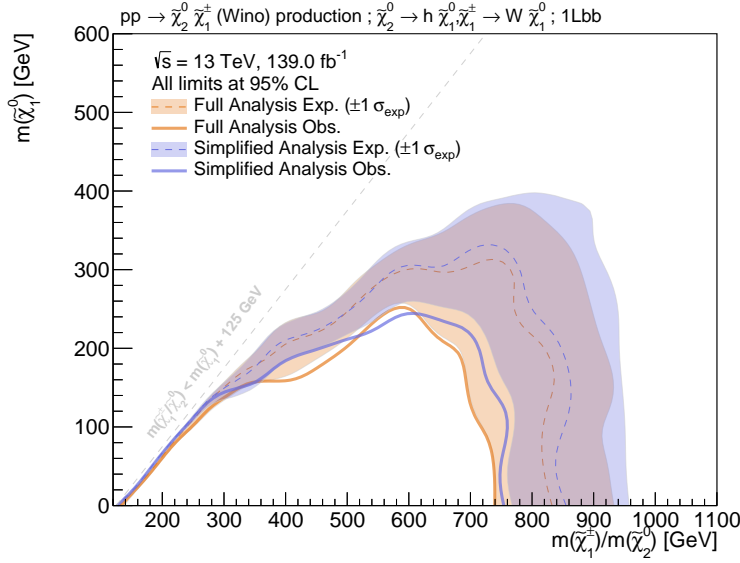
Figure 10.6: Expected and observed exclusion contours obtained with the full likelihood and reconstruction-level inputs (orange) and the simplified likelihood and smeared truth-level inputs (purple). All statistical and systematic uncertainties on the background and signal are considered for the reconstruction-level contours determined using the full likelihood.

herein. In the case of the ATLAS stop search, shown in fig. 10.5(b), significant signal contamination[†] of more than 30% appears in the control regions for many signal models with $m(\tilde{t}_1) < m(\tilde{\chi}_1^0) + m(t)$, thereby breaking one of the base assumptions of the simplified likelihood. In fig. B.5, the impact of applying the simplified likelihood on signal models with significant signal contamination in the region $m(\tilde{t}_1) < m(\tilde{\chi}_1^0) + m(t)$ is shown. In practice, this means that models need to be carefully checked for potential signal contamination in the control regions, and cannot be evaluated using the simplified likelihood in case the signal contamination is found to be too high[§].

10.6 Outlook and future prospects

The simplified likelihood method [289] introduced in this chapter can offer precise and computationally efficient approximations of ATLAS SUSY searches for which the full likelihood in JSON format is available. A publicly available python tool has been developed for the generic conversion of any full likelihood in JSON format into the simplified format introduced herein [290].

The procedure of approximating the statistical model of a search is orthogonal to the truth-level analysis discussed in section 9.4 in the sense that both approximations target a different part of the analysis workflow shown in fig. 9.1. As such, both approaches can be combined into a *simplified analysis* that runs a smeared truth-level analysis in order to determine an estimate for the signal event rates, followed by a simplified statistical inference using the simplified likelihood. Figure 10.6 compares the expected and observed exclusion contours obtained in the full 1ℓ search with those obtained with the simplified version of the search. The agreement between the exclusion contours obtained by both analysis versions is noteworthy, especially given the considerable scope of the two-fold approximation

---

[†]   Since the kinematic properties of the $\tilde{t}_1$ decays drastically change in the parameter region with $m(\tilde{t}_1) < m(\tilde{\chi}_1^0) + m(t)$, this is a kinematic region that the analysis is not designed to be sensitive to. Therefore the CRs are not guaranteed to be free of signal contamination.

[§]   The exact amount of tolerable signal contamination should be explicitly checked on a per-analysis basis. For models exceeding the tolerated amount, the full likelihood may be used instead of the simplified one.

applied in the simplified analysis version. The simplified version of the 1ℓ analysis will be used in the following chapter to enable a computationally efficient reinterpretation of the 1ℓ search in the pMSSM.

As the full likelihood defines the full statistical model (given the observed data) in an analysis, other forms of likelihood simplifications can be thought of. One possible approach worth investigating is the construction of likelihood simplifications using a variable number of nuisance parameters, as opposed to reducing the full set of nuisance parameters to a single one. In such an approach, a principal components analysis can be used to project the full N-dimensional nuisance parameter space onto a number $n \leq N$ principal components maximising the variance of the projected space, i.e. resulting in minimal loss in bin-by-bin correlation information. The n principal components can then be kept separate in a simplified likelihood, while the $N - n$ remaining components can be combined into a *residual* term[†]. A similar approach was already introduced in chapter 7, where the large number of nuisance parameters related to the jet energy resolution (JER) and jet energy scale (JES) uncertainties were reduced to a more manageable set of *effective* nuisance parameters with minimal loss in bin-by-bin correlation information.

Up until very recently, the only way for physicists to re-use ATLAS searches for SUSY outside the collaboration required building approximations of their statistical models based on publicly available lossy projections of the full likelihood. With the recent push by the ATLAS Collaboration to publish the full analysis likelihoods, new approaches for approximating the statistical models are becoming available. In principle, the full likelihood contains all the information necessary for generating a simplified likelihood with a variable degree of simplification, allowing to find an optimal compromise between the desired statistical precision and the required computational efficiency.

[†]   The simplified likelihood introduced in this thesis can be understood as the special case where $n = 0$ is chosen and none of the principal components are kept separate while all N nuisance parameters are combined into a single residual term (taking into account correlations between them).

Part IV

Summary and Outlook

Part V

Appendices

Appendix B

Simplified analysis

The following sections provide additional material on the approximations made in the context of the *simplified analysis* used throughout part III of this thesis. The simplified analysis is composed of truth-level analysis using smeared truth MC datasets, and the simplified likelihood for the statistical inference.

B.1   Truth smearing

The estimated event rates in the exclusion signal regions at truth-level before and after truth smearing are compared with the reconstruction-level event rates in figs. B.1 to B.3. Each one of the 125 signal points from the simplified model signal grid corresponds to one point in the scatter plots. The error bars correspond to the MC statistical uncertainties at truth- and reconstruction-level.

The smearing significantly improves the agreement between truth- and reconstruction-level event rate estimates in all signal region bins. While the lepton reconstruction and identification efficiencies are crucial to provide a good agreement between truth- and reconstruction-level distributions down to the lower bounds of 7 GeV and 6 GeV used for electrons and muons, respectively, the flavour-tagging efficiencies provide the overall agreement in normalisation (since all signal regions require exactly two b-tagged jets in the final state).
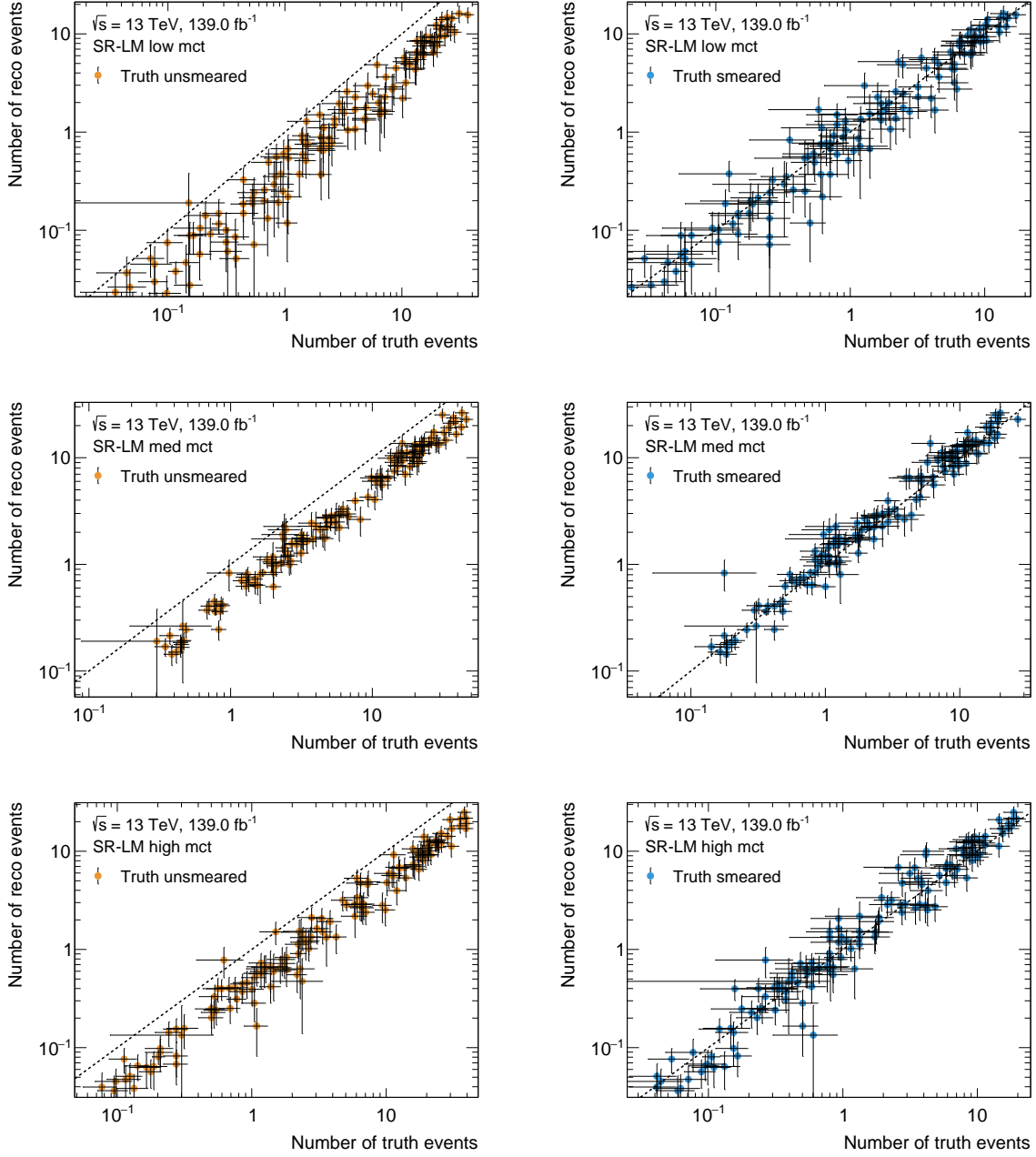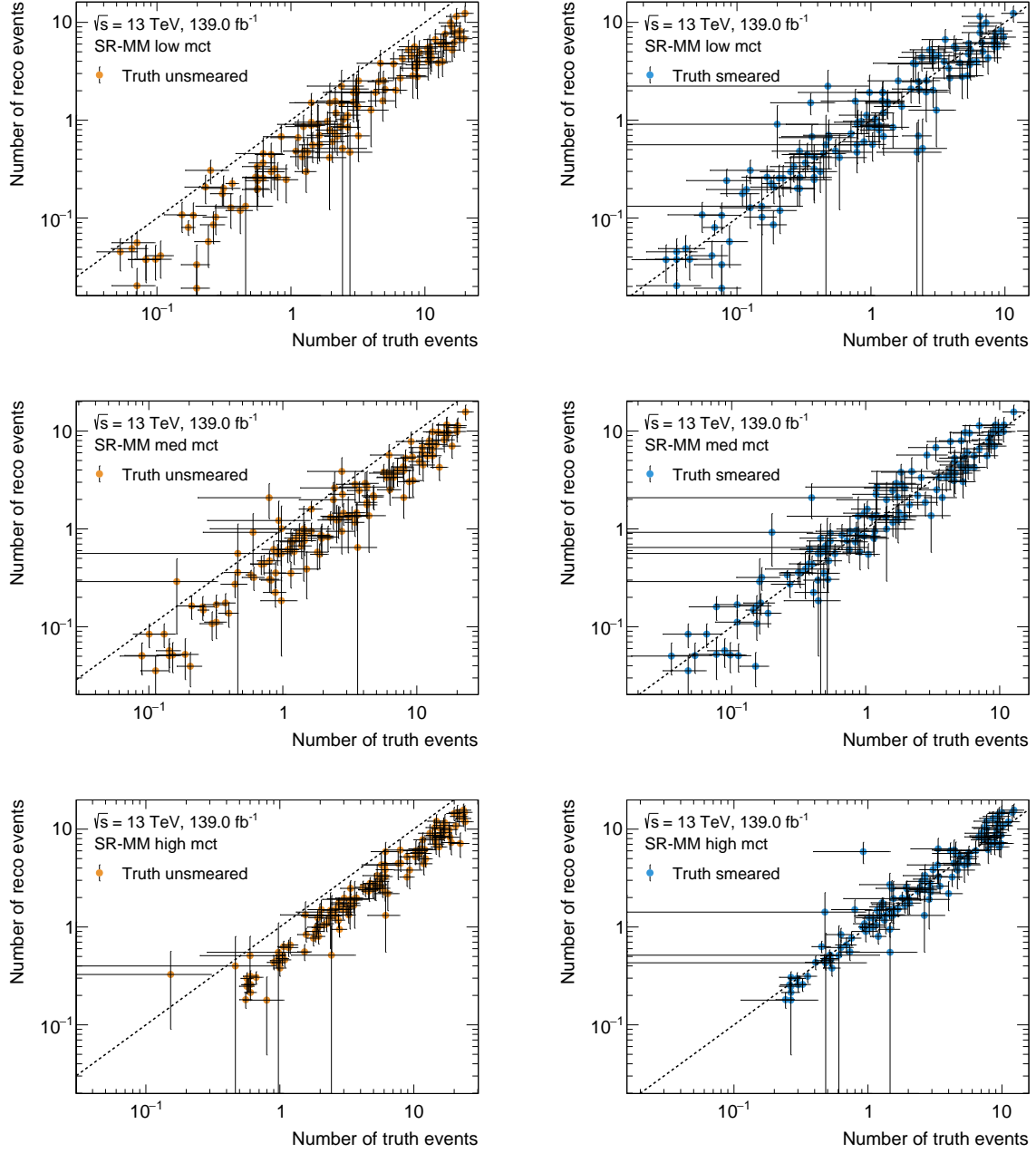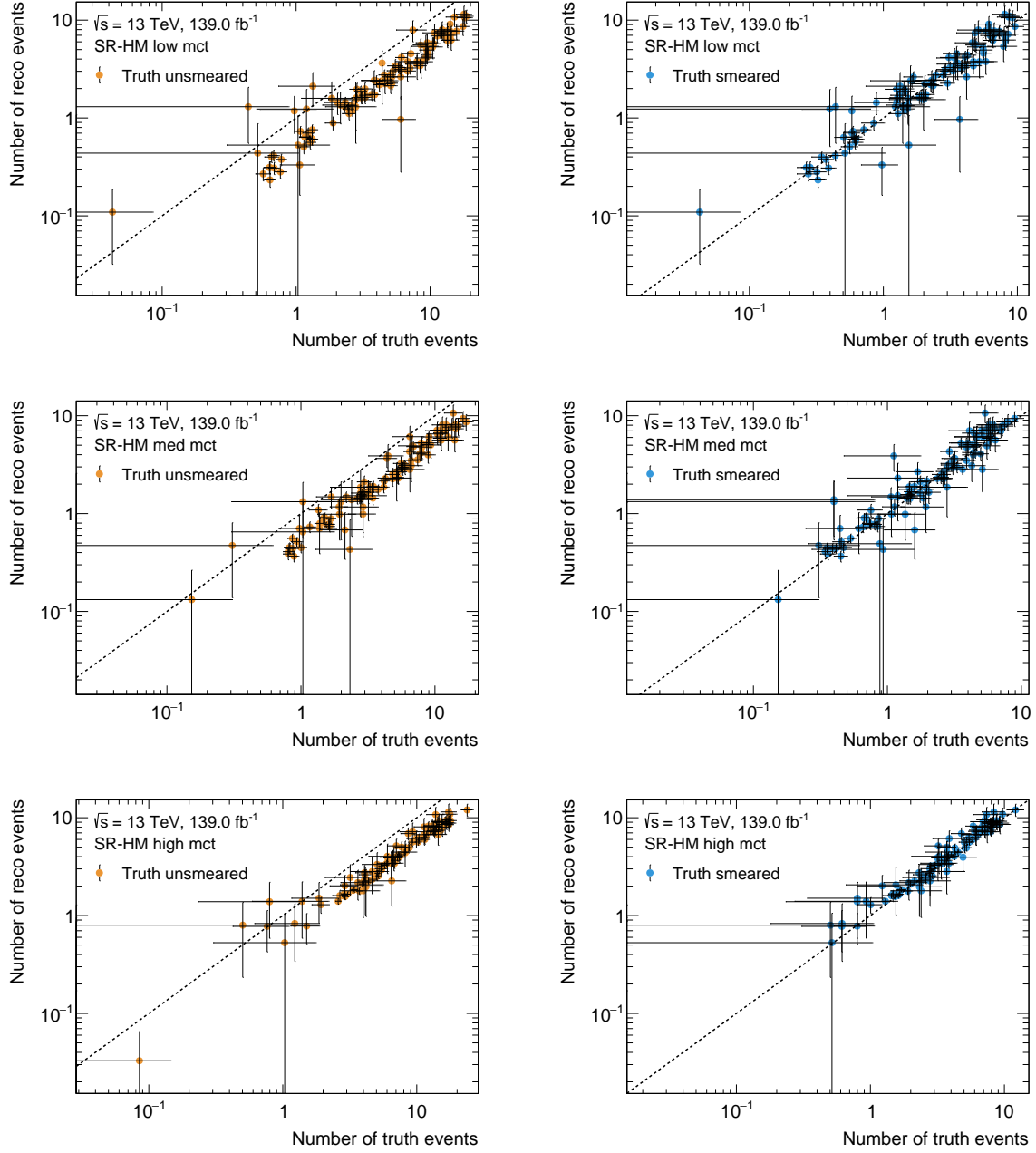
Figure B.1: Comparison of the event rates at truth- and reconstruction-level before (left) and after (right) truth smearing in SR-LM. From top to bottom, the low, medium and high m_{CT} bins are shown. Every single point in the scatter plots represents a single signal model considered in the 1ℓ analysis. Uncertainties include only MC statistical uncertainties.

Figure B.2: Comparison of the event rates at truth- and reconstruction-level before (left) and after (right) truth smearing in SR-MM. From top to bottom, the low, medium and high m_{CT} bins are shown. Every single point in the scatter plots represents a single signal model considered in the 1ℓ analysis. Uncertainties include only MC statistical uncertainties.

Figure B.3: Comparison of the event rates at truth- and reconstruction-level before (left) and after (right) truth smearing in SR-HM. From top to bottom, the low, medium and high m_{CT} bins are shown. Every single point in the scatter plots represents a single signal model considered in the 1ℓ analysis. Uncertainties include only MC statistical uncertainties.

B.2 Simplified likelihood results

Figures B.4 and B.5 highlight the limitations of the simplified likelihood approach using the ATLAS compressed and stop searches, discussed in section 10.5.

Figures B.6 and B.7 directly compare the expected and observed CL_s values obtained using both likelihood configurations for each ATLAS SUSY search considered. Both linear- and log-scale representations are shown, revealing that the simplified likelihood tends to lead to good agreement in the CL_s values around 0.05, while slightly overestimating sensitivity in the region with $CL_s \ll 0.05$, where signal models are in any case being excluded.

(a) With problematic SRs

(b) Without problematic SRs
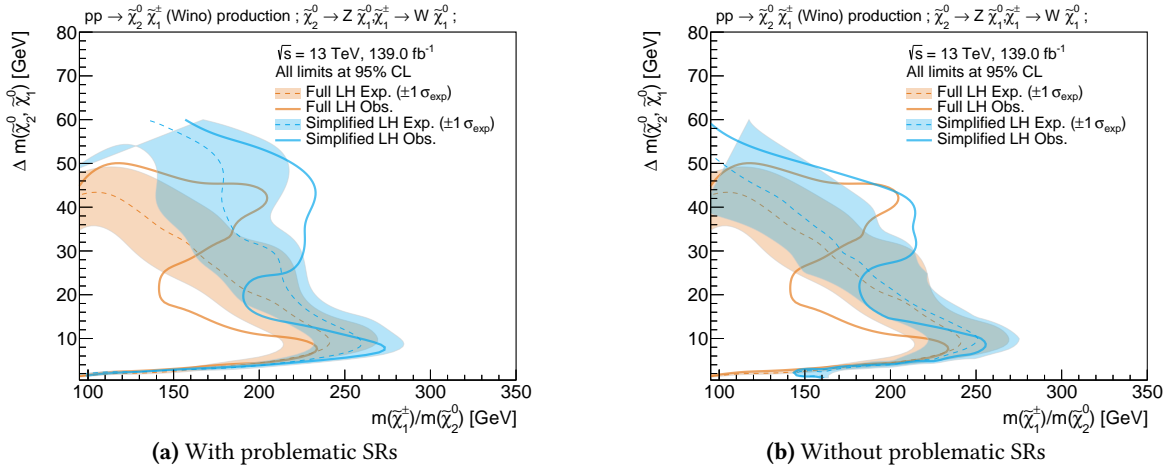
Figure B.4: The contours obtained with the full and simplified likelihoods of the ATLAS compressed search [91] are shown with the problematic signal regions (a) included in the simplified likelihood and (b) removed from it. A noticeable improvement in agreement between the two likelihoods is observed after removing the signal regions responsible for the instabilities discussed in section 10.5.
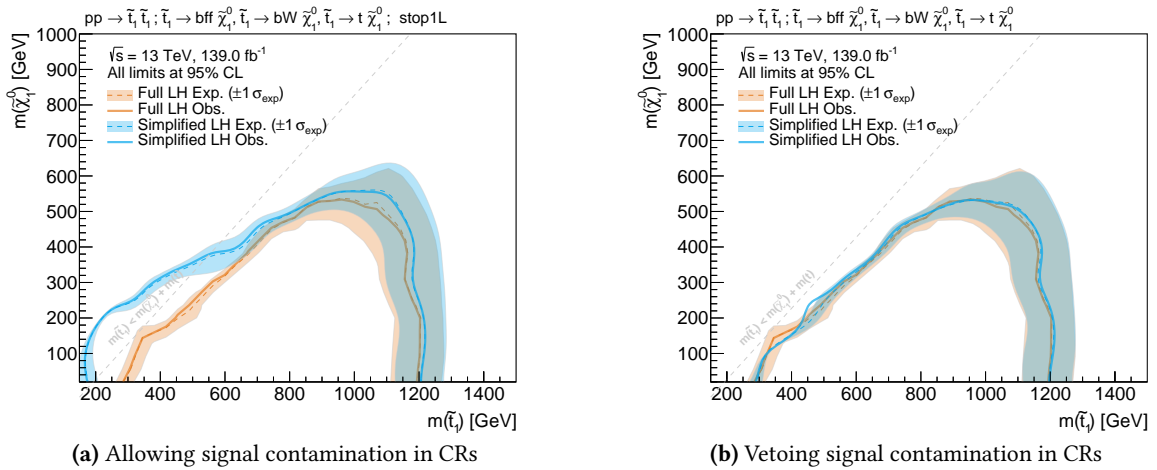

(a) Allowing signal contamination in CRs

(b) Vetoing signal contamination in CRs

Figure B.5: Contours obtained with the full and simplified likelihoods of the ATLAS stop search. In fig. (a) the simplified likelihood is also applied on signal points with $m(\tilde{t}_1) < m(\tilde{\chi}_1^0) + m(t)$, where significant signal contamination in the CRs occurs. In fig. (b), such signal points are removed and thus not evaluated using the simplified likelihood.
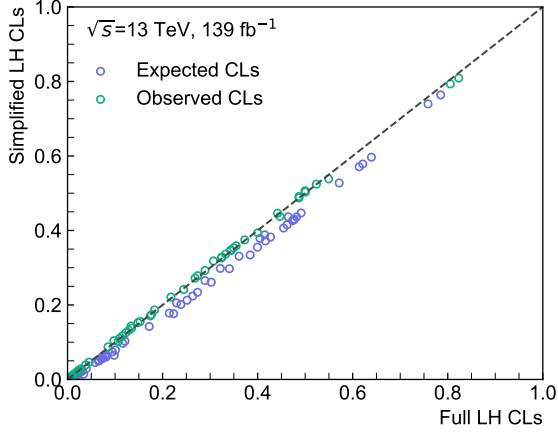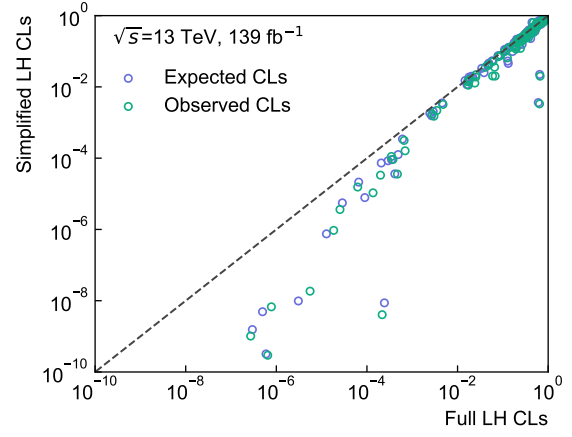
(a) ATLAS sbottom search [294]
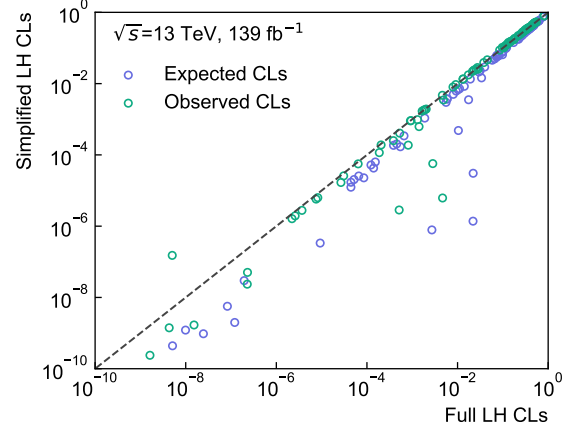
(b) ATLAS sbottom search [294]
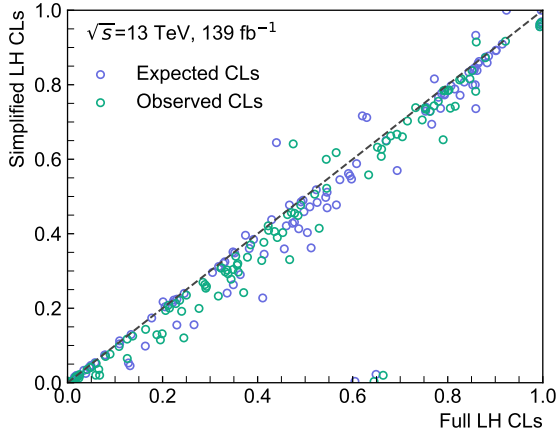
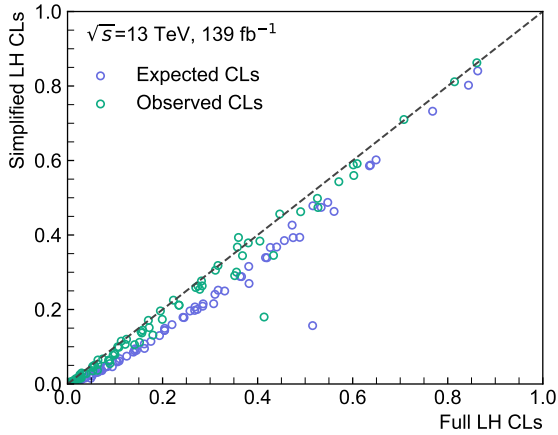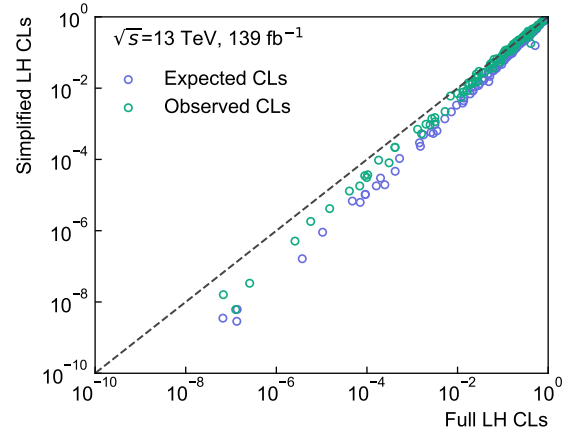**(c)** ATLAS stop search

(d) ATLAS stop search

(e) ATLAS 2ℓ search [260]
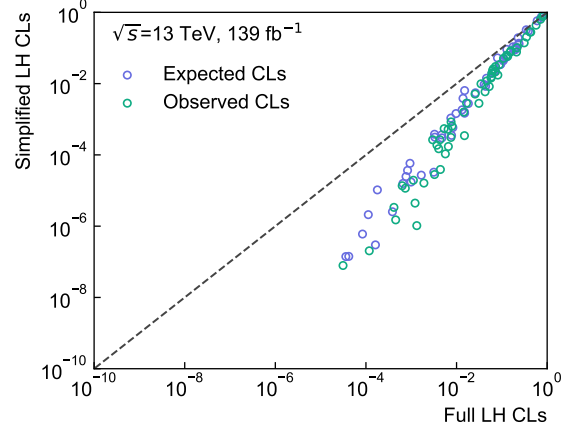
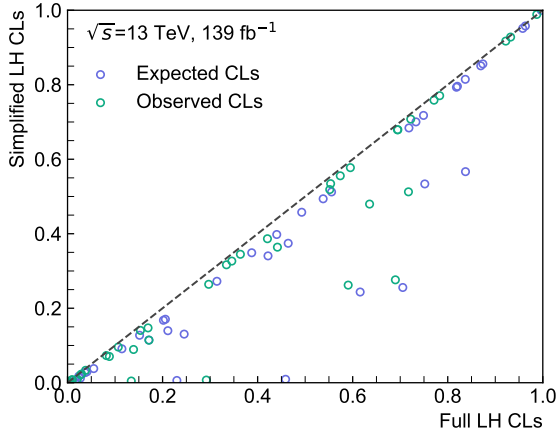**(f)** ATLAS 2ℓ search [260]

Figure B.6: Scatter plots comparing the observed and expected CL_s values obtained using the simplified and the full likelihoods for the same set of signal models originally considered in the various ATLAS SUSY searches. Both linear and logarithmic scale representations are shown on the left- and right-hand side, respectively, illustrating the full range of CL_s values. Apart from the scales, the left-hand and right-hand plots in each row do not differ from each other.
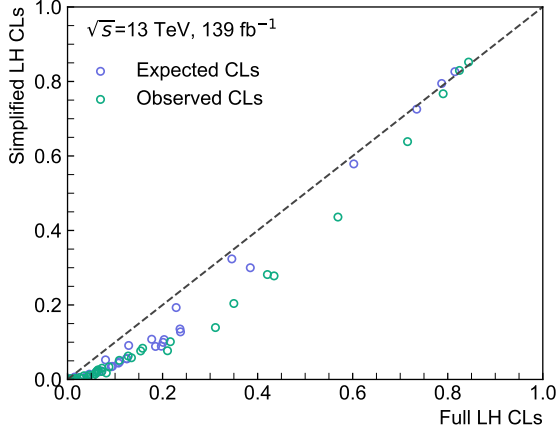
(a) ATLAS direct stau search [293]

(b) ATLAS direct stau search [293]

(c) ATLAS 3ℓ search

(d) ATLAS 3ℓ search

(e) ATLAS compressed search [91]

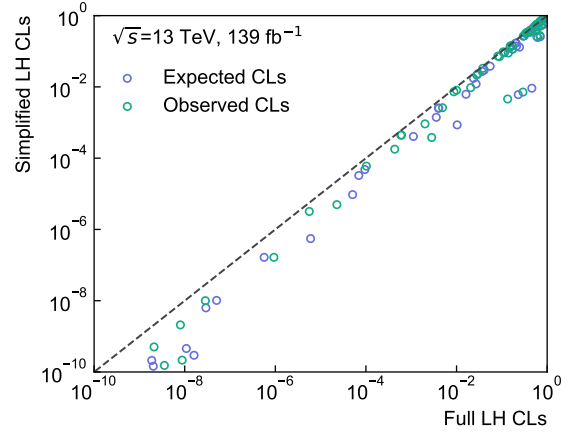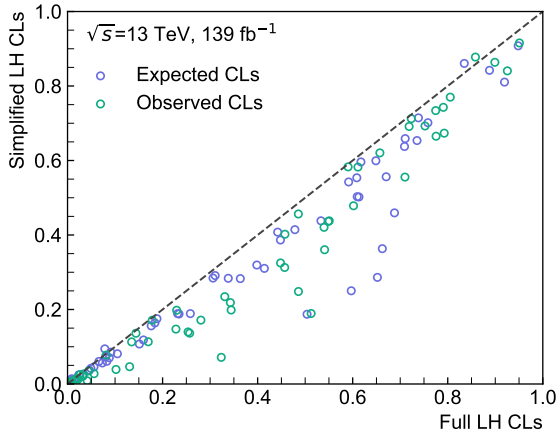**(f)** ATLAS compressed search [91]

Figure B.7: Scatter plots comparing the observed and expected CL_s values obtained using the simplified and the full likelihoods for the same set of signal models originally considered in the various ATLAS SUSY searches. Both linear and logarithmic scale representations are shown on the left- and right-hand side, respectively, illustrating the full range of CL_s values. Apart from the scales, the left-hand and right-hand plots in each row do not differ from each other.
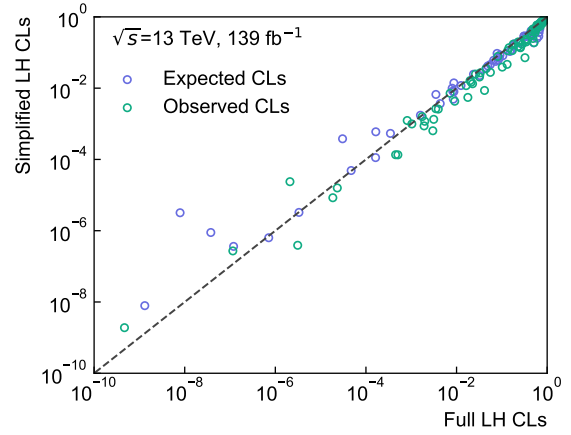
Abbreviations

BSM beyond the Standard Model. 148

CR control region. 148, 153, 155, 195

HEP high energy physics. 147

JER jet energy resolution. 156

JES jet energy scale. 156

MC Monte Carlo. 151, 152, 191–194

pdf probability density function. 152

pMSSM phenomenological Minimal Supersymmetric Standard Model. 145, 147, 156

POI Parameter of Interest. 148, 149

SM Standard Model. 147, 153

SR signal region. 148, 150, 151, 153, 195

SUSY Supersymmetry. 145, 147, 151, 152, 155, 156, 195–197

Bibliography

[1] ATLAS Collaboration, "Observation of a new particle in the search for the Standard Model Higgs boson with the ATLAS detector at the LHC," *Phys. Lett. B* **716** (2012) 1, `arXiv:1207.7214 [hep-ex]`.

[2] CMS Collaboration, "Observation of a new boson at a mass of 125 GeV with the CMS experiment at the LHC," *Phys. Lett. B* **716** (2012) 30, `arXiv:1207.7235 [hep-ex]`.

[3] I. C. Brock and T. Schorner-Sadenius, *Physics at the terascale.* Wiley, Weinheim, 2011. https://cds.cern.ch/record/1354959.

[4] M. E. Peskin and D. V. Schroeder, *An Introduction to quantum field theory.* Addison-Wesley, Reading, USA, 1995. http://www.slac.stanford.edu/~mpeskin/QFT.html.

[5] S. P. Martin, "A Supersymmetry primer," `arXiv:hep-ph/9709356v7 [hep-ph]`. [Adv. Ser. Direct. High Energy Phys.18,1(1998)].

[6] M. Bustamante, L. Cieri, and J. Ellis, "Beyond the Standard Model for Montaneros," in *5th CERN - Latin American School of High-Energy Physics.* 11, 2009. `arXiv:0911.4409 [hep-ph]`.

[7] L. Brown, *The Birth of particle physics.* Cambridge University Press, Cambridge Cambridgeshire New York, 1986.

[8] P. J. Mohr, D. B. Newell, and B. N. Taylor, "CODATA Recommended Values of the Fundamental Physical Constants: 2014," *Rev. Mod. Phys.* **88** no. 3, (2016) 035009, `arXiv:1507.07956 [physics.atom-ph]`.

[9] Particle Data Group, "Review of Particle Physics," *Progress of Theoretical and Experimental Physics* **2020** no. 8, (08, 2020) , https://academic.oup.com/ptep/article-pdf/2020/8/083C01/34673722/ptaa104.pdf. https://doi.org/10.1093/ptep/ptaa104. 083C01.

[10] Super-Kamiokande Collaboration, "Evidence for oscillation of atmospheric neutrinos," *Phys. Rev. Lett.* **81** (1998) 1562–1567, `arXiv:hep-ex/9807003 [hep-ex]`.

[11] Z. Maki, M. Nakagawa, and S. Sakata, "Remarks on the unified model of elementary particles," *Prog. Theor. Phys.* **28** (1962) 870–880. [,34(1962)].

[12] N. Cabibbo, "Unitary symmetry and leptonic decays," *Phys. Rev. Lett.* **10** (Jun, 1963) 531–533. https://link.aps.org/doi/10.1103/PhysRevLett.10.531.

[13] M. Kobayashi and T. Maskawa, "CP Violation in the Renormalizable Theory of Weak Interaction," *Prog. Theor. Phys.* **49** (1973) 652–657.

[14] E. Noether and M. A. Tavel, "Invariant variation problems," `arXiv:physics/0503066`.

[15] J. C. Ward, "An identity in quantum electrodynamics," *Phys. Rev.* **78** (Apr, 1950) 182–182. https://link.aps.org/doi/10.1103/PhysRev.78.182.

[16] Y. Takahashi, "On the generalized ward identity," *Il Nuovo Cimento (1955-1965)* **6** no. 2, (Aug, 1957) 371–375. https://doi.org/10.1007/BF02832514.

[17] G. 'tHooft, "Renormalization of massless yang-mills fields," *Nuclear Physics B* **33** no. 1, (1971) 173 – 199. http://www.sciencedirect.com/science/article/pii/0550321371903956.

[18] J. Taylor, "Ward identities and charge renormalization of the yang-mills field," *Nuclear Physics B* **33** no. 2, (1971) 436 – 444. http://www.sciencedirect.com/science/article/pii/0550321371902975.

[19] A. A. Slavnov, "Ward identities in gauge theories," *Theoretical and Mathematical Physics* **10** no. 2, (Feb, 1972) 99–104. https://doi.org/10.1007/BF01090719.

[20] C. N. Yang and R. L. Mills, "Conservation of isotopic spin and isotopic gauge invariance," *Phys. Rev.* **96** (Oct, 1954) 191–195. https://link.aps.org/doi/10.1103/PhysRev.96.191.

[21] K. G. Wilson, "Confinement of quarks," *Phys. Rev. D* **10** (Oct, 1974) 2445–2459. https://link.aps.org/doi/10.1103/PhysRevD.10.2445.

[22] T. DeGrand and C. DeTar, *Lattice Methods for Quantum Chromodynamics*. World Scientific, Singapore, 2006. https://cds.cern.ch/record/1055545.

[23] S. L. Glashow, "Partial-symmetries of weak interactions," *Nuclear Physics* **22** no. 4, (1961) 579 – 588. http://www.sciencedirect.com/science/article/pii/0029558261904692.

[24] S. Weinberg, "A model of leptons," *Phys. Rev. Lett.* **19** (Nov, 1967) 1264–1266. https://link.aps.org/doi/10.1103/PhysRevLett.19.1264.

[25] A. Salam and J. C. Ward, "Weak and electromagnetic interactions," *Il Nuovo Cimento (1955-1965)* **11** no. 4, (Feb, 1959) 568–577. https://doi.org/10.1007/BF02726525.

[26] C. S. Wu, E. Ambler, R. W. Hayward, *et al.*, "Experimental test of parity conservation in beta decay," *Phys. Rev.* **105** (Feb, 1957) 1413–1415. https://link.aps.org/doi/10.1103/PhysRev.105.1413.

[27] M. Gell-Mann, "The interpretation of the new particles as displaced charge multiplets," *Il Nuovo Cimento (1955-1965)* **4** no. 2, (Apr, 1956) 848–866. https://doi.org/10.1007/BF02748000.

[28] K. Nishijima, "Charge Independence Theory of V Particles*," *Progress of Theoretical Physics* **13** no. 3, (03, 1955) 285–304, https://academic.oup.com/ptp/article-pdf/13/3/285/5425869/13-3-285.pdf. https://doi.org/10.1143/PTP.13.285.

[29] T. Nakano and K. Nishijima, "Charge Independence for V-particles*," *Progress of Theoretical Physics* **10** no. 5, (11, 1953) 581–582, https://academic.oup.com/ptp/article-pdf/10/5/581/5364926/10-5-581.pdf. https://doi.org/10.1143/PTP.10.581.

[30] F. Englert and R. Brout, "Broken symmetry and the mass of gauge vector mesons," *Phys. Rev. Lett.* **13** (Aug, 1964) 321–323. https://link.aps.org/doi/10.1103/PhysRevLett.13.321.

[31] P. W. Higgs, "Broken symmetries and the masses of gauge bosons," *Phys. Rev. Lett.* **13** (Oct, 1964) 508–509. https://link.aps.org/doi/10.1103/PhysRevLett.13.508.

[32] P. W. Higgs, "Spontaneous symmetry breakdown without massless bosons," *Phys. Rev.* **145** (May, 1966) 1156–1163. https://link.aps.org/doi/10.1103/PhysRev.145.1156.

[33] Y. Nambu, "Quasiparticles and Gauge Invariance in the Theory of Superconductivity," *Phys. Rev.* **117** (1960) 648–663. [,132(1960)].

[34] J. Goldstone, "Field Theories with Superconductor Solutions," *Nuovo Cim.* **19** (1961) 154–164.

[35] V. Brdar, A. J. Helmboldt, S. Iwamoto, and K. Schmitz, "Type-I Seesaw as the Common Origin of Neutrino Mass, Baryon Asymmetry, and the Electroweak Scale," *Phys. Rev. D* **100** (2019) 075029, `arXiv:1905.12634 [hep-ph]`.

[36] G. 't Hooft and M. Veltman, "Regularization and renormalization of gauge fields," *Nuclear Physics B* **44** no. 1, (1972) 189 – 213. http://www.sciencedirect.com/science/article/pii/0550321372902799.

[37] G. L. Kane, *The supersymmetric world : the beginnings of the theory.* World Scientific, Singapore River Edge, N.J, 2000.

[38] F. Zwicky, "Die Rotverschiebung von extragalaktischen Nebeln," *Helv. Phys. Acta* **6** (1933) 110–127. https://cds.cern.ch/record/437297.

[39] V. C. Rubin and W. K. Ford, Jr., "Rotation of the Andromeda Nebula from a Spectroscopic Survey of Emission Regions," *Astrophys. J.* **159** (1970) 379–403.

[40] G. Bertone, D. Hooper, and J. Silk, "Particle dark matter: Evidence, candidates and constraints," *Phys. Rept.* **405** (2005) 279–390, `arXiv:hep-ph/0404175`.

[41] D. Clowe, M. Bradac, A. H. Gonzalez, *et al.*, "A direct empirical proof of the existence of dark matter," *Astrophys. J.* **648** (2006) L109–L113, `arXiv:astro-ph/0608407 [astro-ph]`.

[42] A. Taylor, S. Dye, T. J. Broadhurst, *et al.*, "Gravitational lens magnification and the mass of abell 1689," *Astrophys. J.* **501** (1998) 539, `arXiv:astro-ph/9801158`.

[43] C. Bennett *et al.*, "Four year COBE DMR cosmic microwave background observations: Maps and basic results," *Astrophys. J. Lett.* **464** (1996) L1–L4, `arXiv:astro-ph/9601067`.

[44] G. F. Smoot *et al.*, "Structure in the COBE Differential Microwave Radiometer First-Year Maps," *ApJS* **396** (September, 1992) L1.

[45] WMAP Collaboration, "Nine-year Wilkinson Microwave Anisotropy Probe (WMAP) Observations: Final Maps and Results," *ApJS* **208** no. 2, (October, 2013) 20, `arXiv:1212.5225 [astro-ph.CO]`.

[46] WMAP Collaboration, "Nine-year Wilkinson Microwave Anisotropy Probe (WMAP) Observations: Cosmological Parameter Results," *ApJS* **208** no. 2, (October, 2013) 19, `arXiv:1212.5226 [astro-ph.CO]`.

[47] Planck Collaboration, "Planck 2018 results. I. Overview and the cosmological legacy of Planck," *Astron. Astrophys.* **641** (2020) A1, `arXiv:1807.06205 [astro-ph.CO]`.

[48] A. Liddle, *An introduction to modern cosmology; 3rd ed.* Wiley, Chichester, Mar, 2015. https://cds.cern.ch/record/1976476.

[49] Planck Collaboration, "Planck 2018 results. VI. Cosmological parameters," *Astron. Astrophys.* **641** (2020) A6, `arXiv:1807.06209 [astro-ph.CO]`.

[50] H. Georgi and S. L. Glashow, "Unity of all elementary-particle forces," *Phys. Rev. Lett.* **32** (Feb, 1974) 438–441. https://link.aps.org/doi/10.1103/PhysRevLett.32.438.

[51] I. Aitchison, *Supersymmetry in Particle Physics. An Elementary Introduction.* Cambridge University Press, Cambridge, 2007.

[52] Muon g-2 Collaboration, "Final Report of the Muon E821 Anomalous Magnetic Moment Measurement at BNL," *Phys. Rev. D* **73** (2006) 072003, `arXiv:hep-ex/0602035`.

[53] H. Baer and X. Tata, *Weak Scale Supersymmetry: From Superfields to Scattering Events.* Cambridge University Press, 2006.

[54] T. Aoyama *et al.*, "The anomalous magnetic moment of the muon in the Standard Model," *Phys. Rept.* **887** (2020) 1–166, `arXiv:2006.04822 [hep-ph]`.

[55] Muon g-2 Collaboration, "Measurement of the Positive Muon Anomalous Magnetic Moment to 0.46 ppm," *Phys. Rev. Lett.* **126** no. 14, (2021) 141801, `arXiv:2104.03281 [hep-ex]`.

[56] A. Czarnecki and W. J. Marciano, "The Muon anomalous magnetic moment: A Harbinger for 'new physics'," *Phys. Rev. D* **64** (2001) 013014, `arXiv:hep-ph/0102122`.

[57] J. L. Feng and K. T. Matchev, "Supersymmetry and the anomalous magnetic moment of the muon," *Phys. Rev. Lett.* **86** (2001) 3480–3483, `arXiv:hep-ph/0102146`.

[58] S. Coleman and J. Mandula, "All possible symmetries of the s matrix," *Phys. Rev.* **159** (Jul, 1967) 1251–1256. https://link.aps.org/doi/10.1103/PhysRev.159.1251.

[59] R. Haag, J. T. Lopuszanski, and M. Sohnius, "All Possible Generators of Supersymmetries of the s Matrix," *Nucl. Phys.* **B88** (1975) 257. [,257(1974)].

[60] J. Wess and B. Zumino, "Supergauge transformations in four dimensions," *Nucl. Phys. B* **70** (1974) 39.

[61] H. Georgi and S. L. Glashow, "Gauge theories without anomalies," *Phys. Rev. D* **6** (Jul, 1972) 429–431. https://link.aps.org/doi/10.1103/PhysRevD.6.429.

[62] S. Dimopoulos and D. W. Sutter, "The Supersymmetric flavor problem," *Nucl. Phys. B* **452** (1995) 496–512, `arXiv:hep-ph/9504415`.

[63] MEG Collaboration, T. Mori, "Final Results of the MEG Experiment," *Nuovo Cim. C* **39** no. 4, (2017) 325, `arXiv:1606.08168 [hep-ex]`.

[64] H. P. Nilles, "Supersymmetry, Supergravity and Particle Physics," *Phys. Rept.* **110** (1984) 1–162.

[65] A. Lahanas and D. Nanopoulos, "The road to no-scale supergravity," *Physics Reports* **145** no. 1, (1987) 1 – 139. http://www.sciencedirect.com/science/article/pii/0370157387900342.

[66] J. L. Feng, A. Rajaraman, and F. Takayama, "Superweakly interacting massive particles," *Phys. Rev. Lett.* **91** (2003) 011302, `arXiv:hep-ph/0302215`.

[67] S. Y. Choi, J. Kalinowski, G. A. Moortgat-Pick, and P. M. Zerwas, "Analysis of the neutralino system in supersymmetric theories," *Eur. Phys. J. C* **22** (2001) 563–579, `arXiv:hep-ph/0108117`. [Addendum: Eur.Phys.J.C 23, 769–772 (2002)].

[68] Super-Kamiokande Collaboration, "Search for proton decay via $p \to e^+ \pi^0$ and $p \to \mu^+ \pi^0$ in 0.31 megaton-years exposure of the Super-Kamiokande water Cherenkov detector," *Phys. Rev. D95* no. 1, (2017) 012004, `arXiv:1610.03597 [hep-ex]`.

[69] J. R. Ellis, "Beyond the standard model for hill walkers," in *1998 European School of High-Energy Physics*, pp. 133–196. 8, 1998. `arXiv:hep-ph/9812235`.

[70] J. R. Ellis, J. Hagelin, D. V. Nanopoulos, *et al.*, "Supersymmetric Relics from the Big Bang," *Nucl. Phys. B* **238** (1984) 453–476.

[71] D. O. Caldwell, R. M. Eisberg, D. M. Grumm, *et al.*, "Laboratory limits on galactic cold dark matter," *Phys. Rev. Lett.* **61** (Aug, 1988) 510–513. https://link.aps.org/doi/10.1103/PhysRevLett.61.510.

[72] M. Mori, M. M. Nojiri, K. S. Hirata, *et al.*, "Search for neutralino dark matter heavier than the w boson at kamiokande," *Phys. Rev. D* **48** (Dec, 1993) 5505–5518. https://link.aps.org/doi/10.1103/PhysRevD.48.5505.

[73] CDMS Collaboration, D. S. Akerib *et al.*, "Exclusion limits on the WIMP-nucleon cross section from the first run of the Cryogenic Dark Matter Search in the Soudan Underground Laboratory," *Phys. Rev. D* **72** (2005) 052009, arXiv:astro-ph/0507190.

[74] A. Djouadi, J.-L. Kneur, and G. Moultaka, "SuSpect: A Fortran code for the supersymmetric and Higgs particle spectrum in the MSSM," *Comput. Phys. Commun.* **176** (2007) 426–455, arXiv:hep-ph/0211331.

[75] C. F. Berger, J. S. Gainer, J. L. Hewett, and T. G. Rizzo, "Supersymmetry without prejudice," *Journal of High Energy Physics* **2009** no. 02, (Feb, 2009) 023–023. http://dx.doi.org/10.1088/1126-6708/2009/02/023.

[76] J. Alwall, P. Schuster, and N. Toro, "Simplified Models for a First Characterization of New Physics at the LHC," *Phys. Rev.* **D79** (2009) 075020, arXiv:0810.3921 [hep-ph].

[77] L. N. P. W. Group, "Simplified Models for LHC New Physics Searches," *J. Phys.* **G39** (2012) 105005, arXiv:1105.2838 [hep-ph].

[78] D. S. Alves, E. Izaguirre, and J. G. Wacker, "Where the Sidewalk Ends: Jets and Missing Energy Search Strategies for the 7 TeV LHC," *JHEP* **10** (2011) 012, arXiv:1102.5338 [hep-ph].

[79] F. Ambrogi, S. Kraml, S. Kulkarni, *et al.*, "On the coverage of the pMSSM by simplified model results," *Eur. Phys. J. C* **78** no. 3, (2018) 215, arXiv:1707.09036 [hep-ph].

[80] O. Buchmueller and J. Marrouche, "Universal mass limits on gluino and third-generation squarks in the context of Natural-like SUSY spectra," *Int. J. Mod. Phys. A* **29** no. 06, (2014) 1450032, arXiv:1304.2185 [hep-ph].

[81] W. Beenakker, C. Borschensky, M. Krämer, *et al.*, "NNLL-fast: predictions for coloured supersymmetric particle production at the LHC with threshold and Coulomb resummation," *JHEP* **12** (2016) 133, arXiv:1607.07741 [hep-ph].

[82] M. Beneke, M. Czakon, P. Falgari, *et al.*, "Threshold expansion of the $gg(q\bar{q}) \to Q\bar{Q} + X$ cross section at $\mathcal{O}(\alpha_s^4)$," *Phys. Lett. B* **690** (2010) 483, arXiv:0911.5166 [hep-ph].

[83] J. Fiaschi and M. Klasen, "Neutralino-chargino pair production at NLO+NLL with resummation-improved parton density functions for LHC Run II," *Phys. Rev. D* **98** no. 5, (2018) 055014, arXiv:1805.11322 [hep-ph].

[84] B. Fuks, M. Klasen, D. R. Lamprea, and M. Rothering, "Gaugino production in proton-proton collisions at a center-of-mass energy of 8 TeV," *JHEP* **10** (2012) 081, arXiv:1207.2159 [hep-ph].

[85] J. Fiaschi and M. Klasen, "Slepton pair production at the LHC in NLO+NLL with resummation-improved parton densities," *JHEP* **03** (2018) 094, arXiv:1801.10357 [hep-ph].

[86] ATLAS Collaboration, M. Aaboud *et al.*, "Dark matter interpretations of ATLAS searches for the electroweak production of supersymmetric particles in $\sqrt{s}$ = 8 TeV proton-proton collisions," *JHEP* **09** (2016) 175, arXiv:1608.00872 [hep-ex].

[87] ATLAS Collaboration, "Summary of the ATLAS experiment's sensitivity to supersymmetry after LHC Run 1 — interpreted in the phenomenological MSSM," *JHEP* **10** (2015) 134, arXiv:1508.06608 [hep-ex].

[88] ATLAS Collaboration, "Mass reach of the atlas searches for supersymmetry." https://atlas.web.cern.ch/Atlas/GROUPS/PHYSICS/PUBNOTES/ATL-PHYS-PUB-2020-020/fig_23.png, 2020.

[89] CMS Collaboration, "Summary plot moriond 2017." https://twiki.cern.ch/twiki/pub/CMSPublic/SUSYSummary2017/Moriond2017_BarPlot.pdf, 2017.

[90] L. S. W. Group, "Notes lepsusywg/02-04.1 and lepsusywg/01-03.1."
     http://lepsusy.web.cern.ch/lepsusy/, 2004. Accessed: 2021-02-11.

[91] ATLAS Collaboration, "Searches for electroweak production of supersymmetric particles with
     compressed mass spectra in $\sqrt{s}$ = 13 TeV pp collisions with the ATLAS detector," *Phys. Rev. D*
     101 (2020) 052005, `arXiv:1911.12606 [hep-ex]`.

[92] ATLAS Collaboration, "Observation of a new particle in the search for the Standard Model
     Higgs boson with the ATLAS detector at the LHC," *Phys. Lett. B* **716** (2012) 1–29,
     `arXiv:1207.7214 [hep-ex]`.

[93] CMS Collaboration, "Observation of a New Boson at a Mass of 125 GeV with the CMS
     Experiment at the LHC," *Phys. Lett. B* **716** (2012) 30–61, `arXiv:1207.7235 [hep-ex]`.

[94] A. Buckley, "PySLHA: a Pythonic interface to SUSY Les Houches Accord data," *Eur. Phys. J. C*
     75 no. 10, (2015) 467, `arXiv:1305.4194 [hep-ph]`.

[95] CERN, "About cern." https://home.cern/about. Accessed: 2021-01-21.

[96] CERN, "CERN Annual report 2019," tech. rep., CERN, Geneva, 2020.
     https://cds.cern.ch/record/2723123.

[97] O. S. Bruning, P. Collier, P. Lebrun, *et al.*, *LHC Design Report.* CERN Yellow Reports:
     Monographs. CERN, Geneva, 2004. https://cds.cern.ch/record/782076.

[98] M. Blewett and N. Vogt-Nilsen, "Proceedings of the 8th international conference on high-energy
     accelerators, cern 1971. conference held at geneva, 20–24 september 1971." tech. rep., 1971, 1971.

[99] L. R. Evans and P. Bryant, "LHC Machine," *JINST* **3** (2008) S08001. 164 p.
     http://cds.cern.ch/record/1129806. This report is an abridged version of the LHC Design Report
     (CERN-2004-003).

[100] R. Scrivens, M. Kronberger, D. Küchler, *et al.*, "Overview of the status and developments on
      primary ion sources at CERN*," https://cds.cern.ch/record/1382102.

[101] M. Vretenar, J. Vollaire, R. Scrivens, *et al.*, *Linac4 design report*, vol. 6 of *CERN Yellow Reports:*
      Monographs. CERN, Geneva, 2020. https://cds.cern.ch/record/2736208.

[102] E. Mobs, "The CERN accelerator complex - 2019. Complexe des accélérateurs du CERN - 2019,".
      https://cds.cern.ch/record/2684277. General Photo.

[103] ATLAS Collaboration, "The ATLAS Experiment at the CERN Large Hadron Collider," *JINST* **3**
      (2008) S08003.

[104] CMS Collaboration, "The CMS Experiment at the CERN LHC," *JINST* **3** (2008) S08004.

[105] ALICE Collaboration, "The ALICE experiment at the CERN LHC," *JINST* **3** (2008) S08002.

[106] LHCb Collaboration, "The LHCb Detector at the LHC," *JINST* **3** (2008) S08005.

[107] TOTEM Collaboration, "The TOTEM experiment at the CERN Large Hadron Collider," *JINST* **3**
      (2008) S08007.

[108] LHCf Collaboration, "Technical design report of the LHCf experiment: Measurement of photons
      and neutral pions in the very forward region of LHC,".

[109] MoEDAL Collaboration, "Technical Design Report of the MoEDAL Experiment,".

[110] ATLAS Collaboration, "ATLAS Public Results - Luminosity Public Results Run 2,".
      https://twiki.cern.ch/twiki/bin/view/AtlasPublic/LuminosityPublicResultsRun2. Accessed:
      2021-01-17.

[111] ATLAS Collaboration, Z. Marshall, "Simulation of Pile-up in the ATLAS Experiment," *J. Phys. Conf. Ser.* **513** (2014) 022024.

[112] "First beam in the LHC - accelerating science,".
https://home.cern/news/news/accelerators/record-luminosity-well-done-lhc. Accessed: 2021-01-10.

[113] ATLAS Collaboration, "Luminosity determination in *pp* collisions at $\sqrt{s}$ = 13 TeV using the ATLAS detector at the LHC," Tech. Rep. ATLAS-CONF-2019-021, CERN, Geneva, Jun, 2019.
https://cds.cern.ch/record/2677054.

[114] ATLAS Collaboration, "Luminosity determination in pp collisions at $\sqrt{s}$ = 8 TeV using the ATLAS detector at the LHC," *Eur. Phys. J. C* **76** no. 12, (2016) 653, `arXiv:1608.03953 [hep-ex]`.

[115] G. Avoni, M. Bruschi, G. Cabras, *et al.*, "The new LUCID-2 detector for luminosity measurement and monitoring in ATLAS," *Journal of Instrumentation* **13** no. 07, (Jul, 2018) P07017–P07017.
https://doi.org/10.1088/1748-0221/13/07/p07017.

[116] S. van der Meer, "Calibration of the effective beam height in the ISR," Tech. Rep.
CERN-ISR-PO-68-31. ISR-PO-68-31, CERN, Geneva, 1968. https://cds.cern.ch/record/296752.

[117] P. Grafström and W. Kozanecki, "Luminosity determination at proton colliders," *Progress in Particle and Nuclear Physics* **81** (2015) 97 – 148.
http://www.sciencedirect.com/science/article/pii/S0146641014000878.

[118] M. Bajko *et al.*, "Report of the Task Force on the Incident of 19th September 2008 at the LHC,"
Tech. Rep. LHC-PROJECT-Report-1168. CERN-LHC-PROJECT-Report-1168, CERN, Geneva, Mar, 2009. https://cds.cern.ch/record/1168025.

[119] "New schedule for CERN's accelerators and experiments,".
https://home.cern/news/press-release/cern/first-beam-lhc-accelerating-science. Accessed: 2021-01-10.

[120] ATLAS Collaboration, "Luminosity Determination in *pp* Collisions at $\sqrt{s}$ = 7 TeV Using the ATLAS Detector at the LHC," *Eur. Phys. J. C* **71** (2011) 1630, `arXiv:1101.2185 [hep-ex]`.

[121] ATLAS Collaboration, "Improved luminosity determination in pp collisions at $\sqrt{s}$ = 7 TeV using the ATLAS detector at the LHC.," *Eur. Phys. J. C* **73** no. CERN-PH-EP-2013-026, (Feb, 2013) 2518. 27 p. https://cds.cern.ch/record/1517411.

[122] "Record luminosity: well done LHC,". https://home.cern/news/news/accelerators/new-schedule-cerns-accelerators-and-experiments. Accessed: 2021-01-10.

[123] CERN, "New schedule for CERN's accelerators and experiments," November, 2020. https://home.cern/news/news/accelerators/new-schedule-cerns-accelerators-and-experiments. Accessed: 2021-03-12.

[124] A. G., B. A. I., B. O., *et al.*, *High-Luminosity Large Hadron Collider (HL-LHC): Technical Design Report V. 0.1.* CERN Yellow Reports: Monographs. CERN, Geneva, 2017.
https://cds.cern.ch/record/2284929.

[125] J. Pequenao, "Computer generated image of the whole ATLAS detector." Mar, 2008.

[126] ATLAS Collaboration, "ATLAS: Detector and physics performance technical design report. Volume 1,".

[127] J. Pequenao, "Computer generated image of the ATLAS inner detector." Mar, 2008.

[128] ATLAS Collaboration, K. Potamianos, "The upgraded Pixel detector and the commissioning of the Inner Detector tracking of the ATLAS experiment for Run-2 at the Large Hadron Collider," Tech. Rep. ATL-PHYS-PROC-2016-104, CERN, Geneva, Aug, 2016. https://cds.cern.ch/record/2209070. 15 pages, EPS-HEP 2015 Proceedings.

[129] ATLAS IBL Collaboration, "Production and Integration of the ATLAS Insertable B-Layer," *JINST* **13** no. 05, (2018) T05008, `arXiv:1803.00844 [physics.ins-det]`.

[130] ATLAS Collaboration, "ATLAS Insertable B-Layer Technical Design Report," Tech. Rep. CERN-LHCC-2010-013. ATLAS-TDR-19, Sep, 2010. http://cds.cern.ch/record/1291633.

[131] ATLAS Collaboration, "ATLAS b-jet identification performance and efficiency measurement with $t\bar{t}$ events in pp collisions at $\sqrt{s}$ = 13 TeV," *Eur. Phys. J. C* **79** no. 11, (2019) 970, `arXiv:1907.05120 [hep-ex]`.

[132] ATLAS Collaboration, "Particle Identification Performance of the ATLAS Transition Radiation Tracker." ATLAS-CONF-2011-128, 2011. https://cds.cern.ch/record/1383793.

[133] J. Pequenao, "Computer Generated image of the ATLAS calorimeter." Mar, 2008.

[134] J. Pequenao, "Computer generated image of the ATLAS Muons subsystem." Mar, 2008.

[135] S. Lee, M. Livan, and R. Wigmans, "Dual-Readout Calorimetry," *Rev. Mod. Phys.* **90** no. arXiv:1712.05494. 2, (Dec, 2017) 025002. 40 p. https://cds.cern.ch/record/2637852. 44 pages, 53 figures, accepted for publication in Review of Modern Physics.

[136] M. Leite, "Performance of the ATLAS Zero Degree Calorimeter," Tech. Rep. ATL-FWD-PROC-2013-001, CERN, Geneva, Nov, 2013. https://cds.cern.ch/record/1628749.

[137] S. Abdel Khalek *et al.*, "The ALFA Roman Pot Detectors of ATLAS," *JINST* **11** no. 11, (2016) P11013, `arXiv:1609.00249 [physics.ins-det]`.

[138] U. Amaldi, G. Cocconi, A. Diddens, *et al.*, "The real part of the forward proton proton scattering amplitude measured at the cern intersecting storage rings," *Physics Letters B* **66** no. 4, (1977) 390 – 394. http://www.sciencedirect.com/science/article/pii/0370269377900223.

[139] L. Adamczyk, E. Banaś, A. Brandt, *et al.*, "Technical Design Report for the ATLAS Forward Proton Detector," Tech. Rep. CERN-LHCC-2015-009. ATLAS-TDR-024, May, 2015. https://cds.cern.ch/record/2017378.

[140] ATLAS Collaboration, A. R. Martínez, "The Run-2 ATLAS Trigger System," *J. Phys. Conf. Ser.* **762** no. 1, (2016) 012003.

[141] ATLAS Collaboration, *ATLAS level-1 trigger: Technical Design Report.* Technical Design Report ATLAS. CERN, Geneva, 1998. https://cds.cern.ch/record/381429.

[142] ATLAS Collaboration, "Operation of the ATLAS trigger system in Run 2," *JINST* **15** no. 10, (2020) P10004, `arXiv:2007.12539 [physics.ins-det]`.

[143] ATLAS Collaboration, P. Jenni, M. Nessi, M. Nordberg, and K. Smith, *ATLAS high-level trigger, data-acquisition and controls: Technical Design Report.* Technical Design Report ATLAS. CERN, Geneva, 2003. https://cds.cern.ch/record/616089.

[144] ATLAS Collaboration, "The ATLAS Simulation Infrastructure," *Eur. Phys. J. C* **70** (2010) 823–874, `arXiv:1005.4568 [physics.ins-det]`.

[145] T. Gleisberg, S. Hoeche, F. Krauss, *et al.*, "Event generation with SHERPA 1.1," *JHEP* **02** (2009) 007, `arXiv:0811.4622 [hep-ph]`.

[146] A. Buckley *et al.*, "General-purpose event generators for LHC physics," *Phys. Rept.* **504** (2011) 145–233, arXiv:1101.2599 [hep-ph].

[147] V. N. Gribov and L. N. Lipatov, "Deep inelastic e p scattering in perturbation theory," *Sov. J. Nucl. Phys.* **15** (1972) 438–450.

[148] J. Blumlein, T. Doyle, F. Hautmann, *et al.*, "Structure functions in deep inelastic scattering at HERA," in *Workshop on Future Physics at HERA (To be followed by meetings 7-9 Feb and 30-31 May 1996 at DESY).* 9, 1996. arXiv:hep-ph/9609425.

[149] A. Buckley, J. Ferrando, S. Lloyd, *et al.*, "LHAPDF6: parton density access in the LHC precision era," *Eur. Phys. J. C* **75** (2015) 132, arXiv:1412.7420 [hep-ph].

[150] M. Bengtsson and T. Sjostrand, "Coherent Parton Showers Versus Matrix Elements: Implications of PETRA - PEP Data," *Phys. Lett. B* **185** (1987) 435.

[151] S. Catani, F. Krauss, R. Kuhn, and B. R. Webber, "QCD matrix elements + parton showers," *JHEP* **11** (2001) 063, arXiv:hep-ph/0109231.

[152] L. Lonnblad, "Correcting the color dipole cascade model with fixed order matrix elements," *JHEP* **05** (2002) 046, arXiv:hep-ph/0112284.

[153] B. Andersson, G. Gustafson, G. Ingelman, and T. Sjostrand, "Parton Fragmentation and String Dynamics," *Phys. Rept.* **97** (1983) 31–145.

[154] B. Andersson, *The Lund Model.* Cambridge Monographs on Particle Physics, Nuclear Physics and Cosmology. Cambridge University Press, 1998.

[155] D. Amati and G. Veneziano, "Preconfinement as a Property of Perturbative QCD," *Phys. Lett. B* **83** (1979) 87–92.

[156] D. Yennie, S. Frautschi, and H. Suura, "The infrared divergence phenomena and high-energy processes," *Annals of Physics* **13** no. 3, (1961) 379–452. https://www.sciencedirect.com/science/article/pii/0003491661901518.

[157] M. Dobbs and J. B. Hansen, "The HepMC C++ Monte Carlo event record for High Energy Physics," *Comput. Phys. Commun.* **134** (2001) 41–46.

[158] GEANT4 Collaboration, "GEANT4: A Simulation toolkit," *Nucl. Instrum. Meth.* **A506** (2003) 250–303.

[159] ATLAS Collaboration, "The new Fast Calorimeter Simulation in ATLAS," Tech. Rep. ATL-SOFT-PUB-2018-002, CERN, Geneva, Jul, 2018. https://cds.cern.ch/record/2630434.

[160] K. Cranmer, "Practical Statistics for the LHC," in *2011 European School of High-Energy Physics*, pp. 267–308. 2014. arXiv:1503.07622 [physics.data-an].

[161] G. Cowan, K. Cranmer, E. Gross, and O. Vitells, "Asymptotic formulae for likelihood-based tests of new physics," *Eur. Phys. J.* **C71** (2011) 1554, arXiv:1007.1727 [physics.data-an]. [Erratum: Eur. Phys. J.C73,2501(2013)].

[162] ATLAS Collaboration, "Reproduction searches for new physics with the ATLAS experiment through publication of full statistical likelihoods." ATL-PHYS-PUB-2019-029, 2019. https://cds.cern.ch/record/2684863.

[163] ROOT Collaboration, K. Cranmer, G. Lewis, L. Moneta, *et al.*, "HistFactory: A tool for creating statistical models for use with RooFit and RooStats," Tech. Rep. CERN-OPEN-2012-016, New York U., New York, Jan, 2012. https://cds.cern.ch/record/1456844.

[164] W. Verkerke and D. P. Kirkby, "The RooFit toolkit for data modeling," *eConf* **C0303241** (2003) MOLT007, `arXiv:physics/0306116 [physics]`. [,186(2003)].

[165] F. James and M. Roos, "MINUIT: a system for function minimization and analysis of the parameter errors and corrections," *Comput. Phys. Commun.* **10** no. CERN-DD-75-20, (Jul, 1975) 343–367. 38 p. https://cds.cern.ch/record/310399.

[166] L. Moneta, K. Belasco, K. S. Cranmer, *et al.*, "The RooStats Project," *PoS* **ACAT2010** (2010) 057, `arXiv:1009.1003 [physics.data-an]`.

[167] R. Brun and F. Rademakers, "ROOT: An object oriented data analysis framework," *Nucl. Instrum. Meth.* **A389** (1997) 81–86.

[168] I. Antcheva *et al.*, "ROOT — A C++ framework for petabyte data storage, statistical analysis and visualization," *Computer Physics Communications* **182** no. 6, (2011) 1384 – 1385. http://www.sciencedirect.com/science/article/pii/S0010465511000701.

[169] M. Baak, G. J. Besjes, D. Côte, A. Koutsman, J. Lorenz, D. Short, "HistFitter software framework for statistical data analysis," *Eur. Phys. J.* **C75** (2015) 153, `arXiv:1410.1280 [hep-ex]`.

[170] L. Heinrich, M. Feickert, G. Stark, and K. Cranmer, "pyhf: pure-python implementation of histfactory statistical models," *Journal of Open Source Software* **6** no. 58, (2021) 2823. https://doi.org/10.21105/joss.02823.

[171] L. Heinrich, M. Feickert, and G. Stark, "pyhf: v0.6.0," Version 0.6.0. https://github.com/scikit-hep/pyhf.

[172] C. R. Harris, K. J. Millman, S. J. van der Walt, *et al.*, "Array programming with NumPy," *Nature* **585** no. 7825, (Sept., 2020) 357–362. https://doi.org/10.1038/s41586-020-2649-2.

[173] A. Paszke, S. Gross, F. Massa, *et al.*, "Pytorch: An imperative style, high-performance deep learning library," in *Advances in Neural Information Processing Systems 32*, H. Wallach, H. Larochelle, A. Beygelzimer, *et al.*, eds., pp. 8024–8035. Curran Associates, Inc., 2019. http://papers.neurips.cc/paper/9015-pytorch-an-imperative-style-high-performance-deep-learning-library.pdf.

[174] M. Abadi, A. Agarwal, P. Barham, *et al.*, "TensorFlow: Large-scale machine learning on heterogeneous systems," 2015. https://www.tensorflow.org/. Software available from tensorflow.org.

[175] J. Bradbury, R. Frostig, P. Hawkins, *et al.*, "JAX: composable transformations of Python+NumPy programs," Version 0.1.46, 2018. http://github.com/google/jax.

[176] S. S. Wilks, "The large-sample distribution of the likelihood ratio for testing composite hypotheses," *Ann. Math. Statist.* **9** no. 1, (03, 1938) 60–62. https://doi.org/10.1214/aoms/1177732360.

[177] A. Wald, "Tests of statistical hypotheses concerning several parameters when the number of observations is large," *Transactions of the American Mathematical Society* **54** no. 3, (1943) 426–482. https://doi.org/10.1090/S0002-9947-1943-0012401-3.

[178] G. Cowan, "Statistics for Searches at the LHC," in *69th Scottish Universities Summer School in Physics: LHC Physics*, pp. 321–355. 7, 2013. `arXiv:1307.2487 [hep-ex]`.

[179] A. L. Read, "Presentation of search results: the CL_S technique," *J. Phys. G* **28** (2002) 2693.

[180] R. D. Cousins, J. T. Linnemann, and J. Tucker, "Evaluation of three methods for calculating statistical significance when incorporating a systematic uncertainty into a test of the background-only hypothesis for a Poisson process," *Nucl. Instrum. Meth. A* **595** no. 2, (2008) 480, `arXiv:physics/0702156 [physics.data-an]`.

[181] K. Cranmer, "Statistical challenges for searches for new physics at the LHC," in *Statistical Problems in Particle Physics, Astrophysics and Cosmology (PHYSTAT 05): Proceedings, Oxford, UK, September 12-15, 2005*, pp. 112–123. 2005. `arXiv:physics/0511028 [physics.data-an]`. http://www.physics.ox.ac.uk/phystat05/proceedings/files//Cranmer_LHCStatisticalChallenges.ps.

[182] ATLAS Collaboration, "Search for direct pair production of a chargino and a neutralino decaying to the 125 GeV Higgs boson in $\sqrt{s}$ = 8 TeV pp collisions with the ATLAS detector," *Eur. Phys. J. C* **75** (2015) 208, `arXiv:1501.07110 [hep-ex]`.

[183] ATLAS Collaboration, "Search for chargino and neutralino production in final states with a Higgs boson and missing transverse momentum at $\sqrt{s}$ = 13 TeV with the ATLAS detector," *Phys. Rev. D* **100** (2019) 012006, `arXiv:1812.09432 [hep-ex]`.

[184] CMS Collaboration, "Search for electroweak production of charginos and neutralinos in WH events in proton–proton collisions at $\sqrt{s}$ = 13 TeV," *JHEP* **11** (2017) 029, `arXiv:1706.09933 [hep-ex]`.

[185] ATLAS Collaboration, "Search for direct production of electroweakinos in final states with one lepton, missing transverse momentum and a Higgs boson decaying into two b-jets in pp collisions at $\sqrt{s}$ = 13 TeV with the ATLAS detector," *Eur. Phys. J. C* **80** (2020) 691, `arXiv:1909.09226 [hep-ex]`.

[186] ATLAS Collaboration, "Improvements in $t\bar{t}$ modelling using NLO+PS Monte Carlo generators for Run 2." ATL-PHYS-PUB-2018-009, 2018. https://cds.cern.ch/record/2630327.

[187] ATLAS Collaboration, "Modelling of the $t\bar{t}H$ and $t\bar{t}V(V = W, Z)$ processes for $\sqrt{s}$ = 13 TeV ATLAS analyses." ATL-PHYS-PUB-2016-005, 2016. https://cds.cern.ch/record/2120826.

[188] ATLAS Collaboration, "ATLAS simulation of boson plus jets processes in Run 2." ATL-PHYS-PUB-2017-006, 2017. https://cds.cern.ch/record/2261937.

[189] ATLAS Collaboration, "Multi-Boson Simulation for 13 TeV ATLAS Analyses." ATL-PHYS-PUB-2017-005, 2017. https://cds.cern.ch/record/2261933.

[190] J. Alwall, R. Frederix, S. Frixione, *et al.*, "The automated computation of tree-level and next-to-leading order differential cross sections, and their matching to parton shower simulations," *JHEP* **07** (2014) 079, `arXiv:1405.0301 [hep-ph]`.

[191] R. Frederix and S. Frixione, "Merging meets matching in MC@NLO," *JHEP* **12** (2012) 061, `arXiv:1209.6215 [hep-ph]`.

[192] "Parton distributions with LHC data," *Nucl. Phys. B* **867** (2013) 244, `arXiv:1207.1303 [hep-ph]`.

[193] T. Sjöstrand, S. Ask, J. R. Christiansen, *et al.*, "An Introduction to PYTHIA 8.2," *Comput. Phys. Commun.* **191** (2015) 159–177, `arXiv:1410.3012 [hep-ph]`.

[194] ATLAS Collaboration, "ATLAS Pythia 8 tunes to 7 TeV data." ATL-PHYS-PUB-2014-021, 2014. https://cds.cern.ch/record/1966419.

[195] L. Lönnblad and S. Prestel, "Matching tree-level matrix elements with interleaved showers," *JHEP* **03** (2012) 019, `arXiv:1109.4829 [hep-ph]`.

[196] D. J. Lange, "The EvtGen particle decay simulation package," *Nucl. Instrum. Meth. A* **462** (2001) 152.

[197] ATLAS Collaboration, "The Pythia 8 A3 tune description of ATLAS minimum bias and inelastic measurements incorporating the Donnachie–Landshoff diffractive model." ATL-PHYS-PUB-2016-017, 2016. https://cds.cern.ch/record/2206965.

[198] B. Fuks, M. Klasen, D. R. Lamprea, and M. Rothering, "Precision predictions for electroweak superpartner production at hadron colliders with RESUMMINO," *Eur. Phys. J. C* **73** (2013) 2480, `arXiv:1304.0790 [hep-ph]`.

[199] S. Alioli, P. Nason, C. Oleari, and E. Re, "A general framework for implementing NLO calculations in shower Monte Carlo programs: the POWHEG BOX," *JHEP* **06** (2010) 043, `arXiv:1002.2581 [hep-ph]`.

[200] S. Frixione, P. Nason, and G. Ridolfi, "A Positive-weight next-to-leading-order Monte Carlo for heavy flavour hadroproduction," *JHEP* **09** (2007) 126, `arXiv:0707.3088 [hep-ph]`.

[201] P. Nason, "A New method for combining NLO QCD with shower Monte Carlo algorithms," *JHEP* **11** (2004) 040, `arXiv:hep-ph/0409146`.

[202] E. Bothmann *et al.*, "Event generation with Sherpa 2.2," *SciPost Phys.* **7** no. 3, (2019) 034, `arXiv:1905.09127 [hep-ph]`.

[203] NNPDF Collaboration, "Parton distributions for the LHC run II," *JHEP* **04** (2015) 040, `arXiv:1410.8849 [hep-ph]`.

[204] M. Czakon and A. Mitov, "Top++: A program for the calculation of the top-pair cross-section at hadron colliders," *Comput. Phys. Commun.* **185** (2014) 2930, `arXiv:1112.5675 [hep-ph]`.

[205] M. Cacciari, M. Czakon, M. Mangano, *et al.*, "Top-pair production at hadron colliders with next-to-next-to-leading logarithmic soft-gluon resummation," *Phys. Lett. B* **710** (2012) 612–622, `arXiv:1111.5869 [hep-ph]`.

[206] P. Kant, O. M. Kind, T. Kintscher, *et al.*, "HatHor for single top-quark production: Updated predictions and uncertainty estimates for single top-quark production in hadronic collisions," *Comput. Phys. Commun.* **191** (2015) 74–89, `arXiv:1406.4403 [hep-ph]`.

[207] N. Kidonakis, "Two-loop soft anomalous dimensions for single top quark associated production with a W^- or H^-," *Phys. Rev. D* **82** (2010) 054018, `arXiv:1005.4451 [hep-ph]`.

[208] J. M. Campbell and R. K. Ellis, "$t\bar{t}W^{+-}$ production and decay at NLO," *JHEP* **07** (2012) 052, `arXiv:1204.5678 [hep-ph]`.

[209] A. Lazopoulos, T. McElmurry, K. Melnikov, and F. Petriello, "Next-to-leading order QCD corrections to $t\bar{t}Z$ production at the LHC," *Phys. Lett. B* **666** (2008) 62–65, `arXiv:0804.2220 [hep-ph]`.

[210] R. Gavin, Y. Li, F. Petriello, and S. Quackenbush, "FEWZ 2.0: A code for hadronic Z production at next-to-next-to-leading order," `arXiv:1011.3540 [hep-ph]`.

[211] LHC Higgs Cross Section Working Group Collaboration, "Handbook of LHC Higgs Cross Sections: 4. Deciphering the Nature of the Higgs Sector," `arXiv:1610.07922 [hep-ph]`.

[212] ATLAS Collaboration, "Example ATLAS tunes of PYTHIA8, PYTHIA6 and POWHEG to an observable sensitive to Z boson transverse momentum." ATL-PHYS-PUB-2013-017, 2013. https://cds.cern.ch/record/1629317.

[213] ATLAS Collaboration, "Performance of the ATLAS track reconstruction algorithms in dense environments in LHC Run 2," *Eur. Phys. J. C* **77** (2017) 673, `arXiv:1704.07983 [hep-ex]`.

[214] R. Frühwirth, "Application of Kalman filtering to track and vertex fitting," *Nucl. Instrum. Methods Phys. Res., A* **262** no. HEPHY-PUB-503, (Jun, 1987) 444. 19 p. https://cds.cern.ch/record/178627.

[215] T. Cornelissen, M. Elsing, I. Gavrilenko, *et al.*, "The new ATLAS track reconstruction (NEWT)," *J. Phys.: Conf. Ser.* **119** (2008) 032014. https://cds.cern.ch/record/1176900.

[216] ATLAS Collaboration, "Vertex Reconstruction Performance of the ATLAS Detector at $\sqrt{s}$ = 13 TeV." ATL-PHYS-PUB-2015-026, 2015. https://cds.cern.ch/record/2037717.

[217] ATLAS Collaboration, "Reconstruction of primary vertices at the ATLAS experiment in Run 1 proton–proton collisions at the LHC," *Eur. Phys. J. C* **77** (2017) 332, arXiv:1611.10235 [hep-ex].

[218] ATLAS Collaboration, "Topological cell clustering in the ATLAS calorimeters and its performance in LHC Run 1," *Eur. Phys. J. C* **77** (2017) 490, arXiv:1603.02934 [hep-ex].

[219] ATLAS Collaboration, "Electron and photon performance measurements with the ATLAS detector using the 2015–2017 LHC proton–proton collision data," *JINST* **14** (2019) P12006, arXiv:1908.00005 [hep-ex].

[220] ATLAS Collaboration, "Measurement of the photon identification efficiencies with the ATLAS detector using LHC Run 2 data collected in 2015 and 2016," *Eur. Phys. J. C* **79** (2019) 205, arXiv:1810.05087 [hep-ex].

[221] ATLAS Collaboration, "Electron reconstruction and identification in the ATLAS experiment using the 2015 and 2016 LHC proton–proton collision data at $\sqrt{s}$ = 13 TeV," *Eur. Phys. J. C* **79** (2019) 639, arXiv:1902.04655 [hep-ex].

[222] ATLAS Collaboration, "Muon reconstruction performance of the ATLAS detector in proton–proton collision data at $\sqrt{s}$ = 13 TeV," *Eur. Phys. J. C* **76** (2016) 292, arXiv:1603.05598 [hep-ex].

[223] ATLAS Collaboration, "Muon reconstruction and identification efficiency in ATLAS using the full Run 2 pp collision data set at $\sqrt{s}$ = 13 TeV," arXiv:2012.00578 [hep-ex].

[224] M. Cacciari, G. P. Salam, and G. Soyez, "The anti-k_t jet clustering algorithm," *JHEP* **04** (2008) 063, arXiv:0802.1189 [hep-ph].

[225] M. Cacciari, G. P. Salam, and G. Soyez, "FastJet user manual," *Eur. Phys. J. C* **72** (2012) 1896, arXiv:1111.6097 [hep-ph].

[226] M. Cacciari, "FastJet: A Code for fast k_t clustering, and more," in *Deep inelastic scattering. Proceedings, 14th International Workshop, DIS 2006, Tsukuba, Japan, April 20-24, 2006*, pp. 487–490. 2006. arXiv:hep-ph/0607071 [hep-ph]. [,125(2006)].

[227] ATLAS Collaboration, "Jet energy scale and resolution measured in proton-proton collisions at $\sqrt{s}$ = 13 TeV with the ATLAS detector," arXiv:2007.02645 [hep-ex].

[228] M. Cacciari and G. P. Salam, "Pileup subtraction using jet areas," *Phys. Lett. B* **659** (2008) 119–126, arXiv:0707.1378 [hep-ph].

[229] ATLAS Collaboration, "Jet energy measurement with the ATLAS detector in proton–proton collisions at $\sqrt{s}$ = 7 TeV," *Eur. Phys. J. C* **73** (2013) 2304, arXiv:1112.6426 [hep-ex].

[230] ATLAS Collaboration, "Determination of jet calibration and energy resolution in proton–proton collisions at $\sqrt{s}$ = 8 TeV using the ATLAS detector," arXiv:1910.04482 [hep-ex].

[231] ATLAS Collaboration, "Performance of pile-up mitigation techniques for jets in pp collisions at $\sqrt{s}$ = 8 TeV using the ATLAS detector," *Eur. Phys. J. C* **76** (2016) 581, arXiv:1510.03823 [hep-ex].

[232] ATLAS Collaboration, "Optimisation and performance studies of the ATLAS b-tagging algorithms for the 2017-18 LHC run." ATL-PHYS-PUB-2017-013, 2017. https://cds.cern.ch/record/2273281.

[233] ATLAS Collaboration, "ATLAS b-jet identification performance and efficiency measurement with $t\bar{t}$ events in pp collisions at $\sqrt{s}$ = 13 TeV," *Eur. Phys. J. C* **79** (2019) 970, `arXiv:1907.05120 [hep-ex]`.

[234] ATLAS Collaboration, "Measurements of b-jet tagging efficiency with the ATLAS detector using $t\bar{t}$ events at $\sqrt{s}$ = 13 TeV," *JHEP* **08** (2018) 089, `arXiv:1805.01845 [hep-ex]`.

[235] ATLAS Collaboration, "Performance of missing transverse momentum reconstruction with the ATLAS detector using proton–proton collisions at $\sqrt{s}$ = 13 TeV," *Eur. Phys. J. C* **78** (2018) 903, `arXiv:1802.08168 [hep-ex]`.

[236] ATLAS Collaboration, "$E_{\mathrm{T}}^{\mathrm{miss}}$ performance in the ATLAS detector using 2015-2016 LHC p-p collisions," Tech. Rep. ATLAS-CONF-2018-023, CERN, Geneva, Jun, 2018. http://cds.cern.ch/record/2625233.

[237] D. Adams *et al.*, "Recommendations of the Physics Objects and Analysis Harmonisation Study Groups 2014," Tech. Rep. ATL-PHYS-INT-2014-018, CERN, Geneva, Jul, 2014. https://cds.cern.ch/record/1743654.

[238] M. Cacciari, G. P. Salam, and G. Soyez, "The Catchment Area of Jets," *JHEP* **04** (2008) 005, `arXiv:0802.1188 [hep-ph]`.

[239] UA1 Collaboration, "Experimental Observation of Isolated Large Transverse Energy Electrons with Associated Missing Energy at $\sqrt{s}$ = 540 GeV," *Phys. Lett. B* **122** (1983) 103–116.

[240] Aachen-Annecy-Birmingham-CERN-Helsinki-London(QMC)-Paris(CdF)-Riverside-Rome-Rutherford-Saclay(CEN)-Vienna Collaboration, G. Arnison *et al.*, "Further evidence for charged intermediate vector bosons at the SPS collider," *Phys. Lett. B* **129** no. CERN-EP-83-111, (Jun, 1985) 273–282. 17 p. https://cds.cern.ch/record/163856.

[241] U. Baur, "Measuring the W boson mass at hadron colliders," in *Mini-Workshop on Electroweak Precision Data and the Higgs Mass.* 4, 2003. `arXiv:hep-ph/0304266`.

[242] J. Smith, W. L. van Neerven, and J. A. M. Vermaseren, "The Transverse Mass and Width of the W Boson," *Phys. Rev. Lett.* **50** (1983) 1738.

[243] D. R. Tovey, "On measuring the masses of pair-produced semi-invisibly decaying particles at hadron colliders," *JHEP* **04** (2008) 034, `arXiv:0802.2879 [hep-ph]`.

[244] G. Polesello and D. R. Tovey, "Supersymmetric particle mass measurement with the boost-corrected contransverse mass," *JHEP* **03** (2010) 030, `arXiv:0910.0174 [hep-ph]`.

[245] ATLAS Collaboration, "Performance of the missing transverse momentum triggers for the ATLAS detector during Run-2 data taking," *JHEP* **08** (2020) 080, `arXiv:2005.09554 [hep-ex]`.

[246] ATLAS Collaboration, "Performance of algorithms that reconstruct missing transverse momentum in $\sqrt{s}$ = 8 TeV proton-proton collisions in the ATLAS detector," *Eur. Phys. J. C* **77** no. 4, (2017) 241, `arXiv:1609.09324 [hep-ex]`.

[247] ATLAS Collaboration, "ATLAS data quality operations and performance for 2015–2018 data-taking," *JINST* **15** (2020) P04003, `arXiv:1911.04632 [physics.ins-det]`.

[248] ATLAS Collaboration, "Selection of jets produced in 13 TeV proton–proton collisions with the ATLAS detector." ATLAS-CONF-2015-029, 2015. https://cds.cern.ch/record/2037702.

[249] N. Hartmann, "ahoi." https://gitlab.com/nikoladze/ahoi, 2018.

[250] ATLAS Collaboration, "Object-based missing transverse momentum significance in the ATLAS detector," Tech. Rep. ATLAS-CONF-2018-038, CERN, Geneva, Jul, 2018. https://cds.cern.ch/record/2630948.

[251] A. Roodman, "Blind analysis in particle physics," *eConf* **C030908** (2003) TUIT001, `arXiv:physics/0312102`.

[252] W. Buttinger, "Using Event Weights to account for differences in Instantaneous Luminosity and Trigger Prescale in Monte Carlo and Data," tech. rep., CERN, Geneva, May, 2015. https://cds.cern.ch/record/2014726.

[253] ATLAS Collaboration, "Measurement of the Inelastic Proton–Proton Cross Section at $\sqrt{s}$ = 13 TeV with the ATLAS Detector at the LHC," *Phys. Rev. Lett.* **117** (2016) 182002, `arXiv:1606.02625 [hep-ex]`.

[254] ATLAS Collaboration, "A method for the construction of strongly reduced representations of ATLAS experimental uncertainties and the application thereof to the jet energy scale." ATL-PHYS-PUB-2015-014, 2015. https://cds.cern.ch/record/2037436.

[255] J. Bellm *et al.*, "Herwig 7.0/Herwig++ 3.0 release note," *Eur. Phys. J.* **C76** no. 4, (2016) 196, `arXiv:1512.01178 [hep-ph]`.

[256] ATLAS Collaboration, "Simulation of top-quark production for the ATLAS experiment at $\sqrt{s}$ = 13 TeV." ATL-PHYS-PUB-2016-004, 2016. https://cds.cern.ch/record/2120417.

[257] S. Frixione, E. Laenen, P. Motylinski, *et al.*, "Single-top hadroproduction in association with a W boson," *JHEP* **07** (2008) 029, `arXiv:0805.3067 [hep-ph]`.

[258] ATLAS Collaboration Collaboration, "SUSY March 2021 Summary Plot Update," tech. rep., CERN, Geneva, Mar, 2021. http://cds.cern.ch/record/2758782. All figures including auxiliary figures are available at https://atlas.web.cern.ch/Atlas/GROUPS/PHYSICS/PUBNOTES/ATL-PHYS-PUB-2021-007.

[259] CMS Collaboration, "Search for chargino-neutralino production in final states with a Higgs boson and a W boson," Tech. Rep. CMS-PAS-SUS-20-003, CERN, Geneva, 2021. https://cds.cern.ch/record/2758360.

[260] ATLAS Collaboration, "Search for electroweak production of charginos and sleptons decaying into final states with two leptons and missing transverse momentum in $\sqrt{s}$ = 13 TeV pp collisions using the ATLAS detector," *Eur. Phys. J. C* **80** (2020) 123, `arXiv:1908.08215 [hep-ex]`.

[261] G. Apollinari, I. Béjar Alonso, O. Brüning, *et al.*, *High-Luminosity Large Hadron Collider (HL-LHC): Preliminary Design Report*. CERN Yellow Reports: Monographs. CERN, Geneva, 2015. https://cds.cern.ch/record/2116337.

[262] X. Chen, S. Dallmeier-Tiessen, R. Dasler, *et al.*, "Open is not enough," *Nature Physics* **15** no. 2, (Feb, 2019) 113–119. https://doi.org/10.1038/s41567-018-0342-2.

[263] LHC Reinterpretation Forum Collaboration, W. Abdallah *et al.*, "Reinterpretation of LHC Results for New Physics: Status and Recommendations after Run 2," *SciPost Phys.* **9** no. 2, (2020) 022, `arXiv:2003.07868 [hep-ph]`.

[264] ATLAS Collaboration, "RECAST framework reinterpretation of an ATLAS Dark Matter Search constraining a model of a dark Higgs boson decaying to two b-quarks." ATL-PHYS-PUB-2019-032, 2019. https://cds.cern.ch/record/2686290.

[265] K. Cranmer and I. Yavin, "RECAST: Extending the Impact of Existing Analyses," *JHEP* **04** (2011) 038, `arXiv:1010.2506 [hep-ex]`.

[266] D. Dercks, N. Desai, J. S. Kim, *et al.*, "CheckMATE 2: From the model to the limit," *Comput. Phys. Commun.* **221** (2017) 383–418, `arXiv:1611.09856 [hep-ph]`.

[267] M. Drees, H. Dreiner, D. Schmeier, *et al.*, "CheckMATE: Confronting your Favourite New Physics Model with LHC Data," *Comput. Phys. Commun.* **187** (2015) 227–265, arXiv:1312.2591 [hep-ph].

[268] E. Conte, B. Fuks, and G. Serret, "MadAnalysis 5, A User-Friendly Framework for Collider Phenomenology," *Comput. Phys. Commun.* **184** (2013) 222–256, arXiv:1206.1599 [hep-ph].

[269] E. Maguire, L. Heinrich, and G. Watt, "HEPData: a repository for high energy physics data," *J. Phys. Conf. Ser.* **898** no. 10, (2017) 102006, arXiv:1704.05473 [hep-ex].

[270] ATLAS Collaboration, "Simpleanalysis." https://gitlab.cern.ch/atlas-sa/simple-analysis, 2021.

[271] S. Ovyn, X. Rouby, and V. Lemaitre, "DELPHES, a framework for fast simulation of a generic collider experiment," arXiv:0903.2225 [hep-ph].

[272] A. Buckley, J. Butterworth, D. Grellscheid, *et al.*, "Rivet user manual," *Comput. Phys. Commun.* **184** (2013) 2803–2819, arXiv:1003.0694 [hep-ph].

[273] A. Buckley, D. Kar, and K. Nordström, "Fast simulation of detector effects in Rivet," *SciPost Phys.* **8** (2020) 025, arXiv:1910.01637 [hep-ph].

[274] S. Kraml, S. Kulkarni, U. Laa, *et al.*, "SModelS: a tool for interpreting simplified-model results from the LHC and its application to supersymmetry," *Eur. Phys. J. C* **74** (2014) 2868, arXiv:1312.4175 [hep-ph].

[275] F. Ambrogi, S. Kraml, S. Kulkarni, *et al.*, "SModelS v1.1 user manual: Improving simplified model constraints with efficiency maps," *Comput. Phys. Commun.* **227** (2018) 72–98, arXiv:1701.06586 [hep-ph].

[276] ATLAS Collaboration, "Search for direct production of electroweakinos in final states with one lepton, missing transverse momentum and a higgs boson decaying into two *b*-jets in *pp* collisions at $\sqrt{s}$ = 13 tev with the atlas detector," 2021. https://www.hepdata.net/record/ins1755298?version=4.

[277] ATLAS Collaboration, "1lbb-likelihoods-hepdata.tar.gz," 2020. https://www.hepdata.net/record/resource/1408476?view=true.

[278] G. Alguero, S. Kraml, and W. Waltenberger, "A SModelS interface for pyhf likelihoods," arXiv:2009.01809 [hep-ph].

[279] M. D. Goodsell, "Implementation of the ATLAS-SUSY-2019-08 analysis in the MadAnalysis 5 framework (electroweakinos with a Higgs decay into a $b\bar{b}$ pair, one lepton and missing transverse energy; 139 fb^{-1})," *Mod. Phys. Lett. A* **36** no. 01, (2021) 2141006.

[280] J. Y. Araz *et al.*, "Proceedings of the second MadAnalysis 5 workshop on LHC recasting in Korea," *Mod. Phys. Lett. A* **36** no. 01, (2021) 2102001, arXiv:2101.02245 [hep-ph].

[281] M. Feickert, L. Heinrich, G. Stark, and B. Galewsky, "Distributed statistical inference with pyhf enabled through funcX," in *25th International Conference on Computing in High-Energy and Nuclear Physics.* 3, 2021. arXiv:2103.02182 [cs.DC].

[282] R. Chard, Y. Babuji, Z. Li, *et al.*, "funcx: A federated function serving fabric for science," ACM, Jun, 2020. http://dx.doi.org/10.1145/3369583.3392683.

[283] D. Merkel, "Docker: Lightweight linux containers for consistent development and deployment," *Linux J.* **2014** no. 239, (Mar., 2014) .

[284] S. Binet and B. Couturier, "docker & HEP: Containerization of applications for development, distribution and preservation," *J. Phys.: Conf. Ser.* **664** no. 2, (2015) 022007. 8 p. https://cds.cern.ch/record/2134524.

[285] E. R. Gansner and S. C. North, "An open graph visualization system and its applications to software engineering," *SOFTWARE - PRACTICE AND EXPERIENCE* **30** no. 11, (2000) 1203–1233.

[286] E. R. Gansner, Y. Koren, and S. North, "Graph drawing by stress majorization," in *Graph Drawing*, J. Pach, ed., pp. 239–250. Springer Berlin Heidelberg, Berlin, Heidelberg, 2005.

[287] K. Cranmer and L. Heinrich, "Yadage and Packtivity - analysis preservation using parametrized workflows," *J. Phys. Conf. Ser.* **898** no. 10, (2017) 102019, `arXiv:1706.01878 [physics.data-an]`.

[288] ATLAS Collaboration, "Electron and photon energy calibration with the ATLAS detector using 2015–2016 LHC proton–proton collision data," *JINST* **14** (2019) P03017, `arXiv:1812.03848 [hep-ex]`.

[289] E. Schanet, J. M. Lorenz, G. H. Stark, and L. A. Heinrich, "Simplified likelihoods for searches for supersymmetry," tech. rep., CERN, Geneva, Mar, 2021. https://cds.cern.ch/record/2758958.

[290] Schanet, Eric, "simplify," Version 0.1.5. https://github.com/eschanet/simplify.

[291] Schanet, Eric, "SUSY-2019-08 simplified likelihood," Version 0.0.1. https://github.com/eschanet/simplify/blob/master/examples/ANA-SUSY-2019-08/simplify_BkgOnly.json.

[292] P. C. Bryan and M. Nottingham, "Javascript object notation (json) patch," Version RFC 6902, Apr, 2013. https://www.rfc-editor.org/rfc/rfc6902.txt.

[293] ATLAS Collaboration, "Search for direct stau production in events with two hadronic τ-leptons in $\sqrt{s}$ = 13 TeV pp collisions with the ATLAS detector," *Phys. Rev. D* **101** (2020) 032009, `arXiv:1911.06660 [hep-ex]`.

[294] ATLAS Collaboration, "Search for bottom-squark pair production with the ATLAS detector in final states containing Higgs bosons, b-jets and missing transverse momentum," *JHEP* **12** (2019) 060, `arXiv:1908.03122 [hep-ex]`.

[295] W. Porod, "SPheno, a program for calculating supersymmetric spectra, SUSY particle decays and SUSY particle production at e+ e- colliders," *Comput. Phys. Commun.* **153** (2003) 275–315, `arXiv:hep-ph/0301101`.

[296] W. Porod and F. Staub, "SPheno 3.1: Extensions including flavour, CP-phases and models beyond the MSSM," *Comput. Phys. Commun.* **183** (2012) 2458–2469, `arXiv:1104.1573 [hep-ph]`.

[297] S. Heinemeyer, W. Hollik, and G. Weiglein, "FeynHiggs: A Program for the calculation of the masses of the neutral CP even Higgs bosons in the MSSM," *Comput. Phys. Commun.* **124** (2000) 76–89, `arXiv:hep-ph/9812320`.

[298] H. Bahl, T. Hahn, S. Heinemeyer, *et al.*, "Precision calculations in the MSSM Higgs-boson sector with FeynHiggs 2.14," *Comput. Phys. Commun.* **249** (2020) 107099, `arXiv:1811.09073 [hep-ph]`.

[299] T. Hahn, S. Heinemeyer, W. Hollik, *et al.*, "High-Precision Predictions for the Light CP -Even Higgs Boson Mass of the Minimal Supersymmetric Standard Model," *Phys. Rev. Lett.* **112** no. 14, (2014) 141801, `arXiv:1312.4937 [hep-ph]`.

[300] B. C. Allanach, "SOFTSUSY: a program for calculating supersymmetric spectra," *Comput. Phys. Commun.* **143** (2002) 305–331, `arXiv:hep-ph/0104145 [hep-ph]`.

[301] G. Belanger, F. Boudjema, A. Pukhov, and A. Semenov, "MicrOMEGAs 2.0: A Program to calculate the relic density of dark matter in a generic model," *Comput. Phys. Commun.* **176** (2007) 367–382, `arXiv:hep-ph/0607059`.

[302] G. Belanger, F. Boudjema, A. Pukhov, and A. Semenov, "micrOMEGAs: A Tool for dark matter studies," *Nuovo Cim. C* **033N2** (2010) 111–116, `arXiv:1005.4133 [hep-ph]`.

[303]   W. Beenakker, R. Hopker, and M. Spira, "PROSPINO: A Program for the Production of
        Supersymmetric Particles in Next-to-leading Order QCD," Tech. Rep. hep-ph/9611232, Nov,
        1996. https://cds.cern.ch/record/314229. 12 pages, latex, no figures, Complete postscript file and
        FORTRAN source codes available from http://wwwcn.cern.ch/ mspira/prospino/.

[304]   W. Beenakker, M. Klasen, M. Kramer, *et al.*, "The Production of charginos / neutralinos and
        sleptons at hadron colliders," *Phys. Rev. Lett.* **83** (1999) 3780–3783, arXiv:hep-ph/9906298.
        [Erratum: Phys.Rev.Lett. 100, 029901 (2008)].

[305]   ATLAS Collaboration, "Search for long-lived charginos based on a disappearing-track signature
        using 136 fb^{-1} of pp collisions at $\sqrt{s}$ = 13 TeV with the ATLAS detector," Tech. Rep.
        ATLAS-CONF-2021-015, CERN, Geneva, Mar, 2021. https://cds.cern.ch/record/2759676.

[306]   A. Arbey, M. Battaglia, and F. Mahmoudi, "Higgs Production in Neutralino Decays in the MSSM
        - The LHC and a Future e^+e^- Collider," *Eur. Phys. J. C* **75** no. 3, (2015) 108, arXiv:1212.6865
        [hep-ph].

[307]   M. E. Cabrera, J. A. Casas, A. Delgado, *et al.*, "Naturalness of MSSM dark matter," *JHEP* **08**
        (2016) 058, arXiv:1604.02102 [hep-ph].

[308]   N. Arkani-Hamed, G. L. Kane, J. Thaler, and L.-T. Wang, "Supersymmetry and the LHC inverse
        problem," *JHEP* **08** (2006) 070, arXiv:hep-ph/0512190.

[309]   S. Amari, *Differential-Geometrical Methods in Statistics.* Springer New York, New York, NY,
        1985.

[310]   J. Brehmer, K. Cranmer, F. Kling, and T. Plehn, "Better Higgs boson measurements through
        information geometry," *Phys. Rev. D* **95** no. 7, (2017) 073002, arXiv:1612.05261 [hep-ph].

[311]   ATLAS Collaboration, "Summary of the searches for squarks and gluinos using $\sqrt{s}$ = 8 TeV pp
        collisions with the ATLAS experiment at the LHC," *JHEP* **10** (2015) 054, arXiv:1507.05525
        [hep-ex].

[312]   ATLAS Collaboration, "Search for the electroweak production of supersymmetric particles in
        $\sqrt{s}$ = 8 TeV pp collisions with the ATLAS detector," *Phys. Rev. D* **93** (2016) 052002,
        arXiv:1509.07152 [hep-ex].